

CONSISTENT CREEP AND RUPTURE
PROPERTIES FOR CREEP-FATIGUE EVALUATION**MASTER**

C. C. Schultz
Research Specialist
Member ASME

The Babcock & Wilcox Company
Research and Development Division
Alliance, Ohio

The currently accepted practice of using inconsistent representations of creep and rupture behaviors in the prediction of creep-fatigue life is shown to introduce a factor of safety beyond that specified in current ASME Code design rules for 304 stainless steel Class 1 nuclear components.

Accurate predictions of creep-fatigue life for uniaxial tests on a given heat of material are obtained by using creep and rupture properties for that same heat of material. The use of a consistent representation of creep and rupture properties for a minimum strength heat is also shown to provide adequate predictions.

The viability of using consistent properties (either actual or those of a minimum heat) to predict creep-fatigue life thus identifies significant design uses for the results of characterization tests and improved creep and rupture correlations.

INTRODUCTION

The currently accepted practice for creep-fatigue evaluation of nuclear components is based on the use of a combination of creep properties that are representative of average behavior and rupture properties that are representative of minimum behavior. A purpose of this paper is to show that this combination of properties is not representative of actual 304 stainless steel behavior. It is further intended to demonstrate that a direct result of the use of this combination of properties is the introduction of a factor of safety beyond that specified in current ASME Code design

NOTICE

This report was prepared as an account of work sponsored by the United States Government. Neither the United States nor the United States Department of Energy, nor any of their employees, nor any of their contractors, subcontractors, or their employees, makes any warranty, express or implied, or assumes any legal liability or responsibility for the accuracy, completeness or usefulness of any information, apparatus, product or process disclosed, or represents that its use would not infringe privately owned rights.

DISCLAIMER

This report was prepared as an account of work sponsored by an agency of the United States Government. Neither the United States Government nor any agency Thereof, nor any of their employees, makes any warranty, express or implied, or assumes any legal liability or responsibility for the accuracy, completeness, or usefulness of any information, apparatus, product, or process disclosed, or represents that its use would not infringe privately owned rights. Reference herein to any specific commercial product, process, or service by trade name, trademark, manufacturer, or otherwise does not necessarily constitute or imply its endorsement, recommendation, or favoring by the United States Government or any agency thereof. The views and opinions of authors expressed herein do not necessarily state or reflect those of the United States Government or any agency thereof.

DISCLAIMER

Portions of this document may be illegible in electronic image products. Images are produced from the best available original document.

rules for elevated temperature Class 1 nuclear components. In addition, it is intended to show that the use of consistent creep and rupture properties results in creep-fatigue life predictions that are more reasonable than those of the currently accepted practice.

General rules for creep-fatigue evaluation of Class 1 nuclear components are provided in Appendix T of Code Case 1592 of the ASME Boiler and Pressure Vessel Code⁽¹⁾. These rules limit the accumulated creep-fatigue damage on the basis of independently determined accumulated fatigue damage and accumulated creep damage. The accumulated fatigue damage is determined on the basis of the linear cumulative damage model. The accumulated creep damage is based on the time-fractions linear damage model. The interaction of creep damage and fatigue damage is considered by limiting the combined creep-fatigue damage through the use of the bilinear damage envelope of Figure T-1420-2 of Code Case 1592.

The Code Case provides conservatism in the specification of the design fatigue curves by reducing the average continuous cycling fatigue data by a factor of 2 on total strain range or a factor of 20 on life; whichever provides the minimum result. Additional conservatism is provided by specifying the use of the minimum expected stress-to-rupture curves (Figures I-14.6 of Code Case 1592). Finally, conservatism is introduced by requiring that the stress be divided by the factor K' (0.9 for 304 stainless steel) before entering the minimum stress-to-rupture curves.

The use of the time-fractions model to estimate the creep damage requires a detailed time history of the stresses. When inelastic analysis is used to determine this time history, the calculated secondary and peak stresses are quite dependent on the assumed creep behavior of the material. For example, the assumption of low resistance to creep will result in the prediction of rapidly decreasing secondary and peak stresses. Conversely, the assumption of a high resistance to creep results in the prediction of more slowly decreasing secondary and peak stresses. Thus, when secondary and peak stresses are significant, the calculated creep damage can be quite dependent on the assumed creep behavior. In view of this significant dependence of the calculated creep damage on the assumed representation of

creep behavior and the obvious dependence on the assumed stress rupture behavior, it is important to adequately represent both of these responses.

The Code rules specify that the minimum expected stress rupture behavior shall be the basis for calculating creep damage. However, the Code rules do not provide any guidance as to the creep behavior to be assumed in the determination of the detailed time history of the stresses. Accepted current practice dictates the assumption of creep behavior that is representative of average behavior.

An evaluation of limited creep and rupture data for 304 stainless steel indicates the potential existence of a simple one-to-one relationship between the creep deformation and stress rupture behaviors. Specifically, low resistance to creep deformation is usually accompanied by low resistance to rupture; and high resistance to creep deformation is usually accompanied by high resistance to rupture. Thus, the currently accepted practice results in the assumption of potentially inconsistent representations of creep and stress rupture behaviors. The use of this inconsistent representation implicitly introduces an undefined factor of safety beyond that specified in the Code rules.

Two approaches to eliminating this use of inconsistent representations of creep and rupture behaviors are considered. The first approach is based on the assumption of the existence of the above described simple one-to-one relationship between the creep deformation and stress rupture behaviors. To evaluate this approach, life predictions are made for simple uniaxial strain-controlled fatigue tests, with tensile hold-periods, using the combination of minimum creep deformation behavior and minimum stress rupture behavior. A comparison to published experimental results indicates that this approach provides conservative life estimates that are within a factor of about 5 of the observed life.

The second approach assumes the availability of both creep and rupture data for the actual heat of material to be used in construction. To evaluate this approach, life predictions are made for the same uniaxial strain-controlled cyclic tests as above. However, previously observed

creep and rupture data for these same heats are utilized in the life predictions. This approach provides life predictions that are within a factor of about ± 2 of the observed lives.

RELATIONSHIP BETWEEN THE CREEP AND RUPTURE BEHAVIORS

Creep and stress-rupture data for several heats of 304 stainless steel are examined to determine if a relationship exists between the creep and rupture behaviors. Consideration of this relationship is not new. For example, Monkman and Grant⁽²⁾ considered this same relationship. However, their intent was to estimate rupture life on the basis of minimum creep rate data. The basis of the present evaluation is a comparison of the creep strength (stress required to attain a specified minimum creep rate) and the stress rupture strength (stress required for rupture in a specified time) after normalization with respect to published averages. The average minimum creep rate is as defined in the Nuclear Systems Materials Handbook (NSMH)⁽³⁾. The average stress-rupture curves were derived from the same data base⁽⁴⁾ used to develop the minimum expected stress rupture curves of Code Case 1592.

Previously published creep and stress rupture data for four heats of 304 stainless steel are considered. This data is for heats 55697⁽⁵⁾, 346845⁽⁶⁾, 9T2796⁽⁷⁾, and 8043813⁽⁸⁾. Previously published hold-time fatigue data is also available for each of these four heats. Creep and stress rupture data from eight additional heats previously tested at the Babcock & Wilcox Company are also considered. Hold-time fatigue data is not available for any of these heats.

In Figures 1 through 4, stress rupture and minimum creep rate data at 1100°F (593°C) for heats 55697, 347845, 9T2796, and 8043813 are compared to average data. Stress rupture and minimum creep rate data at 1200°F (649°C) for heat 55697 is compared to average data in Figure 5. This data and similar data at 1200°F (649°C) for the eight heats tested by the Babcock & Wilcox Company was used to develop Figures 6 through 8. Figures 6 through 8 present a comparison of creep strength to the rupture strength for each heat after normalization with respect to the published averages.

In Figure 6, the creep strength is defined as the stress required to obtain a minimum creep rate of 1 percent per 10^2 hours; and the rupture strength is defined as the stress for rupture in 10^3 hours. In Figures 7 and 8 longer time strengths are compared as defined in those figures. Note that the definitions of creep strength and rupture strength used in each of Figures 6 to 8 result in a comparison of creep and rupture behaviors at approximately equal stresses for the published average behavior. That is, the deformation and failure responses are being compared at comparable stress levels.

Also shown in each of Figures 6 through 8 is the combination of average creep strength and minimum rupture strength that represents the currently accepted creep-fatigue evaluation procedure.

The solid line, shown in each of Figures 6 through 8, represents a simple one-to-one relationship between the creep and rupture strengths. The data of those figures indicates that this straightforward relationship is a reasonable approximation for 304 stainless steel. With respect to the calculated creep damage, most of the data falls to the conservative side of the one-to-one line. Thus, for the present purpose, it appears reasonable to assume that an "average" heat may be represented by using 100 percent of the average creep strength and 100 percent of the average rupture strength. Similarly, a minimum strength heat can be represented by 100 percent of the minimum creep strength and 100 percent of the minimum rupture strength.

The NSMH doesn't provide a representation of minimum creep behavior; thus, it is necessary to define the minimum creep strength as a percentage of the average creep strength. A comparison of the minimum and average rupture strengths indicates that the minimum rupture strength is approximately 75 percent of the average rupture strength (this percentage does vary as a function of rupture time). The minimum creep strength is then considered to be represented as 75 percent of the average creep strength.

HOLD-TIME FATIGUE LIFE

Fatigue life reduction factors are commonly used to illustrate the effect of hold-time on fatigue life. The fatigue life reduction (FLR) factor is defined as the ratio of the life (measured in cycles) for continuous cycling conditions to the life (measured in cycles) for hold-time conditions at the same strain range.

Analytically predicted FLR factors are compared to published experimental results for uniaxial strain-controlled cyclic tests with tensile hold-periods. The experimental results considered are for heat 55697 tested at 1200°F (649°C) with a strain range of 1/2 percent; and heats 346845, 9T2796, and 8043813 all tested at 1100°F (593°C) with a strain range of 1 percent. All experimental results were obtained from a tabulated summary in reference 9.

Basis of FLR Factor Predictions

Analytical predictions are based on the following combinations of creep deformation and stress rupture behaviors:

- o Creep deformation and stress rupture behaviors observed for the actual heats subsequently tested in hold-time fatigue.
- o Minimum expected creep deformation and stress rupture behaviors.
- o Currently accepted practice; i.e., average creep deformation behavior and the minimum expected stress rupture behavior.

The representation of average creep behavior was obtained from the NSMH. The form of this representation is

$$\dot{\epsilon}^c = \dot{\epsilon}_x (1 - e^{-st}) + \dot{\epsilon}_t (1 - e^{-rt}) + \dot{\epsilon}_M t$$

In the above equation, $\dot{\epsilon}_t$ is defined as a function of $\dot{\epsilon}_M$; while r , s , ϵ_x , and $\dot{\epsilon}_M$ are defined as functions of stress and temperature. For convenience, it is assumed that the form of representing both the observed and minimum creep behaviors is the same as above.

To simplify the representation of the minimum creep behavior (i.e., creep strength of 75 percent of average), the NSMH average minimum creep rate is first approximated. For example, at 1200°F (649°C)

$$\dot{\epsilon}_M = 2.8 \times 10^{-37} \sigma^{7.57}$$

The minimum creep rate corresponding to 75 percent of the average creep strength at 1200°F (649°C) is then

$$\dot{\epsilon}_{M_{\min}} = 2.47 \times 10^{-36} \sigma^{7.57}$$

This representation of $\dot{\epsilon}_{M_{\min}}$ is then substituted into the NSMH creep equation without further alterations. Thus, the first primary creep term is unaffected, and the second primary creep term is affected only in that $\dot{\epsilon}_M$ is modified.

The observed minimum creep rate for each heat tested in hold-time fatigue is represented as

$$\dot{\epsilon}_{M_{\text{obs}}} = A \sigma^N$$

As in the case of the representation of the minimum behavior, the NSMH creep equation is modified by simply replacing $\dot{\epsilon}_M$ as above.

The specification of the stress range presents some difficulty. Data of reference 9 indicates that the stress range is dependent on the duration of the hold-time. Some of this data is shown in Figure 9 to illustrate this variation. An additional variation from heat-to-heat is also apparent in Figure 9. These variations with both hold-time and heat are not adequately understood to permit their consideration. It is assumed that the cyclic hardening characteristics provided in the NSMH

permits an adequate representation of the stress range for all heats and for all hold-time durations. In some cases, where available data indicates a significant difference from the NSMH data, actual stress range data is also considered. A final simplification is that the stress range will be assumed constant from cycle to cycle.

The minimum rupture data and the interaction of creep damage and fatigue damage are assumed as specified in Code Case 1592. The fatigue lives for continuous cycling conditions are assumed as reported in reference 9. At 1200°F (649°C) with a strain range of 1/2 percent, the continuous cycling fatigue life was reported as 13,624 cycles. At 1100°F (593°C) with a strain range of 1 percent, the life was reported as 3,225 cycles.

Comparison of Predicted and Observed Lives

Heat 55697. This heat was tested at 1200°F (649°C) with a strain range of 1/2 percent. Predicted FLR factors are compared to the experimentally determined FLR factors in Figure 10. The FLR factors predicted on the basis of the previously observed creep and rupture behaviors⁽⁵⁾ (see Figure 5) provides excellent agreement with the observed FLR factors. Note that maximum stresses (half of the stress range near half-life) of 20,500 psi (141 MPa) and 23,000 psi (159 MPa) were considered. The lower value represents the NSMH cyclic hardening data. The higher value represents observed data⁽⁹⁾ at short hold-times (1 minute). The FLR factors predicted on the basis of consistent properties of a minimum strength heat (i.e., minimum creep and minimum rupture) are seen to provide considerable conservatism throughout the range of hold-times for which data is available. The FLR factors predicted on the basis of current practice (i.e., average creep and minimum rupture) provide considerably more conservatism, especially at the longer hold-times.

In Figure 11, the Code-specified factor of 1/0.9 on stress has been considered in the predicted FLR factors. This factor on stress results in increasing the predicted FLR factors by a factor of approximately 1.5 to 2.

The predicted FLR factors shown in Figure 12 consider the full conservatism specified in Code Case 1592. Specifically, the fatigue damage is determined using the design fatigue curves of the Code Case in addition to the use of the factor of 1/0.9 on stress.

Table 1 compares the observed and predicted FLR factors for many of the data points reported in Figures 10 to 12. The predicted FLR factors were determined using the observed stress range, as well as the previously observed creep and rupture behaviors. It should again be noted that the observed stress range was assumed constant throughout each test and is representative of that observed near the half-life of each test.

It is of interest to note that the data from this heat (55697) was that used by Campbell⁽¹⁰⁾ in the development of the Code damage interaction envelope (Figure T-1420-2 of Code Case 1592). This partially explains the success of the present predictions, since Campbell's damage interaction envelope was used in the determination of these FLR factors.

Heat 346845. This heat was tested at 1100°F (593°C) with a strain range of 1 percent. The FLR factors shown in Figure 13 are best estimates; i.e., no conservatism is explicitly introduced. The predictions based on previously observed creep and rupture behaviors⁽⁶⁾ (see Figure 2) and the NSMH hardening characteristics show excellent agreement with the experimental data. FLR factors are also predicted using maximum stresses of 36,750 psi (253 MPa) and 28,400 psi (196 MPa). The higher stress is representative of that observed during the test with a hold-time of 1 minute. The lower stress is representative of that observed during the test with a 1 hour hold-time. The FLR factors predicted on the basis of consistent properties for a minimum strength heat (i.e., minimum creep and minimum rupture behaviors) again provides conservatism throughout the range of conditions tested. Similarly, the predictions based on current practice (i.e., average creep and minimum rupture) provides considerable conservatism throughout.

In Figure 14 the factor of 1/0.9 on stress is introduced in the prediction of all FLR factors. In Figure 15 both of the Code-intended factors for conservatism are introduced in the predicted FLR factors.

Table 2 compares the observed and predicted FLR factors for most of the data points reported in Figures 13 through 15. These predictions are based on the stress range observed near mid-life for each individual test.

Heat 9T2796. This heat was also tested at 1100°F (593°C) with a strain range of 1 percent. The FLR factors of Figure 16, predicted on the basis of previously observed⁽⁷⁾ (see Figure 3) creep and rupture behaviors, are in general non-conservative by a factor of about 1.5. The introduction of the factor of 1/0.9 on stress results in a reasonable upper bound to the data, as shown in Figure 17. The representation of a heat of minimum strength provides marginal conservatism for all except the test with a 3-hour hold-time, as shown in Figure 16. As seen in Figure 17, the use of the factor of 1/0.9 on stress with the minimum heat representation provides conservatism throughout the test range. When the full Code-intended conservatism is introduced, as shown in Figure 18, the conservatism is quite considerable. As demonstrated in Table 3, the use of the observed stress range results in very good correlation with the exception of the data with hold-times of 1 and 3 hours.

Heat 8043813. This heat was also tested at 1100°F (593°C) with a strain range of 1 percent. As seen in Figure 19, the hold-time fatigue response of this heat is atypical in that the observed FLR factor does not exhibit the expected increase with increasing hold-time. When the FLR factors are predicted using the observed stress range, conservative results are obtained throughout the test range, as shown in Table 4. The use of the NSMH hardening characteristics and the previously observed creep and rupture behaviors⁽⁸⁾ results in the generally non-conservative predictions of Figure 19. Introduction of the factor of 1/0.9 on stress still results in a non-conservative prediction, as seen in Figure 20. The minimum heat representation and the currently accepted practice both provide conservative results without the introduction of either of the Code-intended factors of safety, as illustrated in Figure 19. In Figure 21 the full Code-intended conservatism has been considered.

Code Safety Factors

Figure 22 illustrates the relative effects of the Code-specified factors of safety at 1100°F (593°C) at a strain range of 1 percent. In that figure the predicted FLR factors are based on consistent properties for a minimum strength heat.

Relaxation

Curve fits of the relaxation behavior observed during the hold-time fatigue testing of heats 55697⁽¹⁰⁾ and 346845⁽¹¹⁾ have been published. These curve fits represent the behavior observed near half-life. Figures 23 and 24 illustrate this observed relaxation behavior as derived from the reported curve fits. Included in those figures are first cycle and near half-life predictions based on the NSMH creep equation and also the modification of that equation to represent the actual observed minimum creep rate (i.e., the equation as modified to predict the previously discussed FLR factors). The initial (time = 0) stress of each of the curves in both Figures 23 and 24 represents the actual observed maximum stress (i.e., half of the stress range near half-life).

The poor comparison between observed and predicted stress histories indicates that the classical creep strain hardening model grossly over-estimates the hardening, and/or the NSMH creep equation (both original and modified forms) is unable to predict relaxation behavior. Note that in the case of heat 346845 the limits of applicability of the NSMH equation have been exceeded by a considerable margin. However, as a result of creep hardening, the effect of primary creep should be nearly exhausted at half-life, such that the secondary creep rate should be completely governing. This being the case, the modified NSMH equation should be quite adequate, even at the high stresses experienced in heat 346845.

Life predictions have been made for heats 55697 and 346845 based on the actual observed stress history and the actual time-to-rupture data. These predictions are compared to the actual data in Table 5. At short hold-times, these predictions are quite good; but at longer hold-times,

the predictions become quite non-conservative. A graphical comparison of the predicted and observed lives is shown in Figure 25. The broken lines represent factors of ± 2 . The indication that the predicted life is relatively independent of the duration of the hold-time reflects the observed rapid stress relaxation.

DISCUSSION

It is thought that any procedure to predict creep-fatigue life should focus on just that goal. In addition, it is thought that any and all necessary factors of safety should be explicitly provided within Code design rules.

The correlations presented in this paper adequately demonstrate that the currently accepted practice of predicting creep-fatigue life implicitly results in an additional margin of safety not specified in the Code design rules. Figure 26 presents a direct comparison of predicted and observed hold-time fatigue lives for the four heats of 304 stainless steel under discussion. In this comparison, the currently accepted practice (i.e., average creep behavior and minimum rupture behavior) has been applied with no explicit margins of safety introduced. Note that this practice implicitly introduces a factor of safety that ranges from 2 to 10.

As observed in Figures 1 through 5, the four subject heats of 304 stainless steel represent rather diverse strengths during standard constant-load creep-rupture tests. Similarly, rather considerable differences in resistance to hold-time fatigue failure are seen in Figures 10, 13, 16, and 19. In Figures 27 and 28, direct comparisons are made of predicted and observed hold-time fatigue lives. In both figures the predictions are based on the observed creep and rupture behaviors without the assumption of any explicit factors of safety. In Figure 27 the observed stress range was used in the predictions. Figure 28 reflects the use of the NSMH hardening characteristics. In either case, the predictions are within a factor of roughly ± 2 of the observed data. Considering the diverse strengths of the four heats, this is thought to

represent excellent correlation. Of even more interest is the apparent capability to predict the diverse dependence of the FLR factor on hold-time duration, as demonstrated in Figures 10, 13, and 16. The flat response of heat 8043813 seen in Figure 19 was not predicted. It would be of considerable interest to see data for longer hold-times for this heat to determine at what point the FLR factor would begin the characteristic increase.

This demonstrated capability to predict creep-fatigue life on the basis of observed creep and rupture behaviors appears to satisfy the goal of a predictive method much more adequately than does the currently accepted practice. In particular, this approach assures the use of consistent representations of creep and rupture behaviors. This approach then affords the opportunity to specify well defined, meaningful factors of safety that are consistent from heat to heat.

The required long time and high cost of developing creep and rupture data for the actual heats of material to be used in construction would usually prohibit the use of this approach to creep-fatigue evaluation. However, this approach could become viable if the current efforts to develop procedures to characterize the long-time elevated temperature properties of individual heats of material by short-time test results are successful. The potential usefulness of this approach to creep-fatigue evaluation is thus considered to provide significant justification for the continued development of these so-called characterization tests.

A reasonable alternative to the requirement of using the actual creep and rupture data appears to be the use of consistent representations of creep and rupture behaviors for a minimum strength heat. The data shown in Figures 6 through 8 at least appears to support the existence of a consistent correlation between creep and rupture strengths. The existence of the correlation obviates the necessity to load-up the factor of safety within the predictive procedure by using inconsistent creep and rupture properties. The previously discussed predictions based on consistent properties for a minimum strength heat are illustrated in Figure 29 as a direct comparison of predicted and observed hold-time

fatigue lives. With the exception of the datum point representing the 3-hour hold-time test for heat 9T2796, this approach provides conservative predictions that are within a factor of about 5 of the observed data.

This latter approach to creep-fatigue evaluation is perhaps more attractive than that based on the use of actual properties simply in that there is no need to attempt to characterize individual heats. It is thought that the potential of this approach is sufficient to justify a more in-depth evaluation of the relationship between creep behavior and rupture behavior for all materials approved for use in Code Case 1592.

CONCLUSION

No attempt has been made to make the judgement as to what specific factors of safety should be embodied in Code design rules for the creep-fatigue evaluation of Class 1 nuclear components. Instead, the intent has simply been to demonstrate that the currently accepted practice for predicting creep-fatigue life in 304 stainless steel components introduces a factor of safety beyond that specified in current Code design rules. It has been shown that this additional factor of safety is the direct result of the use of inconsistent representations of creep and rupture behaviors.

In addition, it has been demonstrated that the use of either actual creep and rupture data for the particular heats of material to be used in construction or a consistent representation for a minimum strength heat provides an adequate basis for predicting the creep-fatigue life of 304 stainless steel components.

It is thus concluded that the use of consistent properties (either actual properties or those of a minimum heat) provides a base to which Code-specified factors of safety may more reasonably be applied.

It is further concluded that the viability of using actual properties or those of a minimum heat provides significant justification for the continued development of procedures for characterization testing

and for an in-depth evaluation of the relationship between the creep and rupture behaviors for all materials approved for use in Code Case 1592.

REFERENCES

1. ASME Boiler and Pressure Vessel Code, Case Interpretations, Code Case 1592-7, American Society of Mechanical Engineers, New York, 1976.
2. F. C. Monkman and N. J. Grant, "An Empirical Relationship Between Rupture Life and Minimum Creep Rate in Creep-Rupture Tests", Deformation and Fracture at Elevated Temperatures, The M.I.T. Press, Cambridge, Massachusetts, 1956, pp 91-103, N. J. Grant and A. W. Mullendore, ed.
3. "Nuclear Systems Materials Handbook, Vol. 1 - Design Data", TID 26666, Vol. 1, Hanford Engineering Development Laboratory, Richland, Washington, 1974.
4. R. A. Moen, Hanford Engineering Development Laboratory, Richland, Washington, private communication.
5. L. D. Blackburn, "Isochronous Stress-Strain Curves for Austenitic Stainless Steels", The Generation of Isochronous Stress-Strain Curves, American Society of Mechanical Engineers, New York, 1972, pp 15-48.
6. V. K. Sikka, et al, "Heat-to-Heat Variation in Creep Properties of Types 304 and 316 Stainless Steels", Journal of Pressure Vessel Technology, Vol. 97, No. 4, November 1975, pp 243-251.
7. C. C. Schultz, "5.3 Investigations of Creep Failure Under Uniaxial and Multiaxial Conditions", High-Temperature Structural Design Program Semiannual Progress Report for Period Ending December 31, 1975, Oak Ridge National Laboratory ORNL-5136, July 1976, pp 71-85.
8. R. W. Swindeman and C. E. Pugh, Creep Studies on Type 304 Stainless Steel (Heat 8043813) Under Constant and Varying Loads, Oak Ridge National Laboratory ORNL-TM-4427, June 1974.
9. D. R. Diercks and D. T. Raske, "Statistical Analysis and Regression Fit of Elevated-Temperature Low-Cycle Fatigue Data on Type 304 Stainless Steel", Mechanical Properties Test Data for Structural Materials Quarterly Progress Report for Period Ending April 30, 1976, Oak Ridge National Laboratory ORNL-5150, June 1976, pp 3-34.
10. R. D. Campbell, "Creep/Fatigue Interaction Correlation for 304 Stainless Steel Subjected to Strain-Controlled Cycling with Hold Times at Peak Strain", American Society for Mechanical Engineers, 71-PVP-6, 1971.

11. P. S. Maiya and S. Majumdar, "Elevated-Temperature Low-Cycle Fatigue Behavior of Different Heats of Type 304 Stainless Steel", Metallurgical Transactions, Vol. 8A, No. 11, November 1977, pp 1651-1660.

TABLE 1. COMPARISON OF PREDICTED AND OBSERVED FATIGUE
LIFE REDUCTION FACTORS AND CYCLIC LIVES FOR HEAT 55697 TESTED AT 1200°F (649°C)

Predictions Based on Observed Creep and Rupture Data

Hold Time (min)	Strain Range (%)	Stress ⁽¹⁾ Amplitude psi (MPa)	Observed		Predicted	
			Fatigue Life Reduction Factor	Cycles to Failure	Fatigue Life Reduction Factor	Cycles to Failure
1	0.49	23,000 (159)	3.52	3,869	4.76	2,861
	0.49	23,700 (163)	2.55	5,351	--	--
10	0.49	20,090 (139)	8.00	1,703	7.78	1,751
	0.49	21,880 (151)	7.95	1,713	--	--
30	0.49	21,400 (148)	11.20	1,216	--	--
	0.48	20,900 (144)	15.81	862	13.29	1,025
60	0.49	19,900 (137)	13.69	995	13.99	975

(1) Data from reference 10.

TABLE 2. COMPARISON OF PREDICTED AND OBSERVED FATIGUE
LIFE REDUCTION FACTORS AND CYCLIC LIVES FOR HEAT 346845 TESTED AT 1100°F (593°C)

Predictions Based on Observed Creep and Rupture Data

Hold Time (min)	Strain Range (%)	Stress (1) Amplitude psi (MPa)	Observed		Predicted	
			Fatigue Life Reduction Factor	Cycles to Failure	Fatigue Life Reduction Factor	Cycles to Failure
1	1.00	36,750 (507)	1.06	3,034	1.81	1,785
5	1.04	33,100 (456)	1.45	2,225	--	--
	1.03	34,800 (480)	1.45	2,222	2.95	1,093
10	0.99	32,900 (454)	1.77	1,826	3.04	1,061
60	1.00	28,400 (392)	4.20	767	3.20	1,009

(1) Data from reference 11.

TABLE 3. COMPARISON OF PREDICTED AND OBSERVED FATIGUE
LIFE REDUCTION FACTORS AND CYCLIC LIVES FOR HEAT 9T2796 TESTED AT 1100°F (593°C)

Predictions Based on Observed Creep and Rupture Data

Hold Time (min)	Strain Range (%)	Stress ⁽¹⁾ Amplitude psi (MPa)	Observed		Predicted	
			Fatigue Life Reduction Factor	Cycles to Failure	Fatigue Life Reduction Factor	Cycles to Failure
1	1.05	34,600 (239)	1.77	1,824		
	1.01	36,800 (254)	2.75	1,171		
	1.01	35,400 (244)	2.43	1,328		
	1.01	37,600 (259)	1.99	1,619	2.87	1,123
	1.01	36,200 (250)	1.93	1,670		
	1.01	33,200 (229)	1.43	2,255	2.21	1,461
	1.00	34,900 (241)	2.11	1,528		
	1.00	36,200 (250)	2.07	1,560		
	1.00	37,300 (257)	2.02	1,593		
	1.00	35,000 (242)	1.94	1,664		
	1.00	35,200 (243)	1.84	1,748		
	1.00	34,600 (239)	1.54	2,099		
0.99	37,300 (258)	2.61	1,235			
	*Average	35,700 (246)	1.97	1,638	2.61	1,235
10	1.01	33,300 (230)	5.83	553		
	1.01	32,900 (227)	5.07	636		
	1.00	33,500 (231)	4.57	706		
	*Average	33,200 (229)	5.10	632	4.45	724
15	1.00	32,000 (221)	4.84	666	4.77	676
60	0.99	29,700 (205)	9.54	338	6.72	480
180	1.02	32,400 (224)	18.97	170	10.79	299
600	1.03	28,300 (195)	15.21	212	14.66	220
	1.00	31,500 (217)	12.80	252	15.97	202

*Fatigue Life Reduction Factor calculated on the basis of the peak stress representing the average of the reported peak stresses.

TABLE 4. COMPARISON OF PREDICTED AND OBSERVED FATIGUE
LIFE REDUCTION FACTORS AND CYCLIC LIVES FOR HEAT 8043813 TESTED AT 1100°F (593°C)

Predictions Based on Observed Creep and Rupture Data

Hold Time (min)	Strain Range (%)	Stress Amplitude psi (MPa)	Observed		Predicted	
			Fatigue Life Reduction Factor	Cycles to Failure	Fatigue Life Reduction Factor	Cycles to Failure
0.6	1.00	39,100 (270)	1.95	1,650	2.02	1,596
6	1.01	38,200 (263)	1.89	1,708	4.42	729
	1.00	37,500 (259)	2.07	1,555	4.09	788
30	1.00	35,200 (243)	2.05	1,574	5.31	607

TABLE 5. PREDICTED FATIGUE LIFE REDUCTION FACTORS
AND CYCLIC LIVES BASED ON OBSERVED AND PREDICTED RELAXATION

Predictions Based on Observed Rupture Data

Heat 55697 Tested at 1200°F (649°C) and Heat 346845 Tested at 1100°F (593°C)

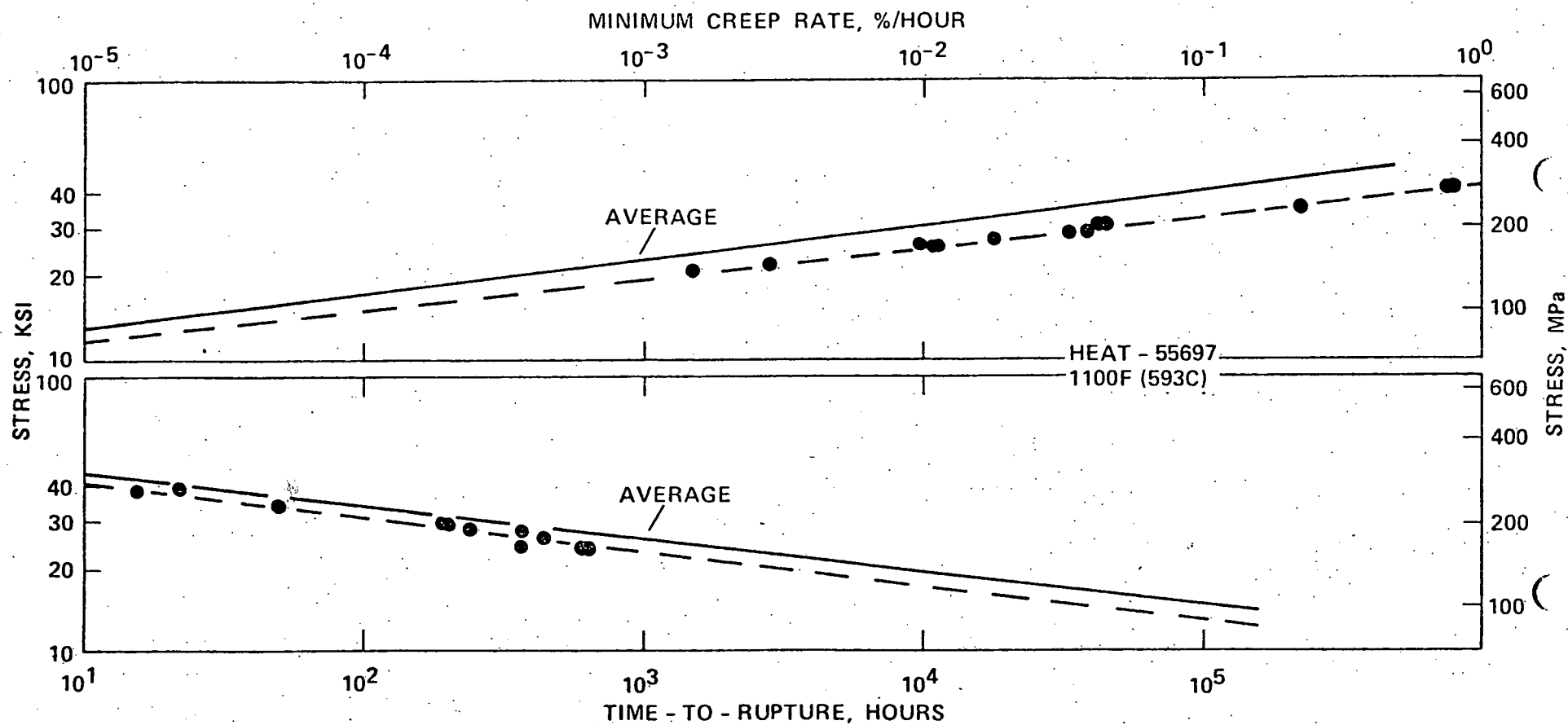
Hold Time (min)	Strain Range (%)	Observed		Predicted		Observed	
		Fatigue Life Reduction Factor	Cycles to Failure	Predicted Relaxation ⁽¹⁾	Fatigue Life Reduction Factor	Cycles to Failure	Fatigue Life Reduction Factor
<u>HEAT 55697</u>							
1	0.49	3.52	3,869	4.76	2,861	3.69	3,695
	0.49	2.55	5,351				
10	0.49	8.00	1,703	7.78	1,751	5.65	2,410
	0.49	7.95	1,713				
30	0.49	11.20	1,216				
	0.48	15.81	862	13.29	1,025	5.67	2,401
60	0.49	13.69	995	13.99	975	6.56	2,076
<u>HEAT 346845</u>							
1	1.00	1.06	3,304	1.81	1,785	1.31	2,468
5	1.04	1.45	2,225				
	1.03	1.45	2,222	2.95	1,093	1.48	2,184
10	0.99	1.77	1,826	3.04	1,061	1.50	2,147
60	1.00	4.20	767	3.20	1,009	1.17	2,753

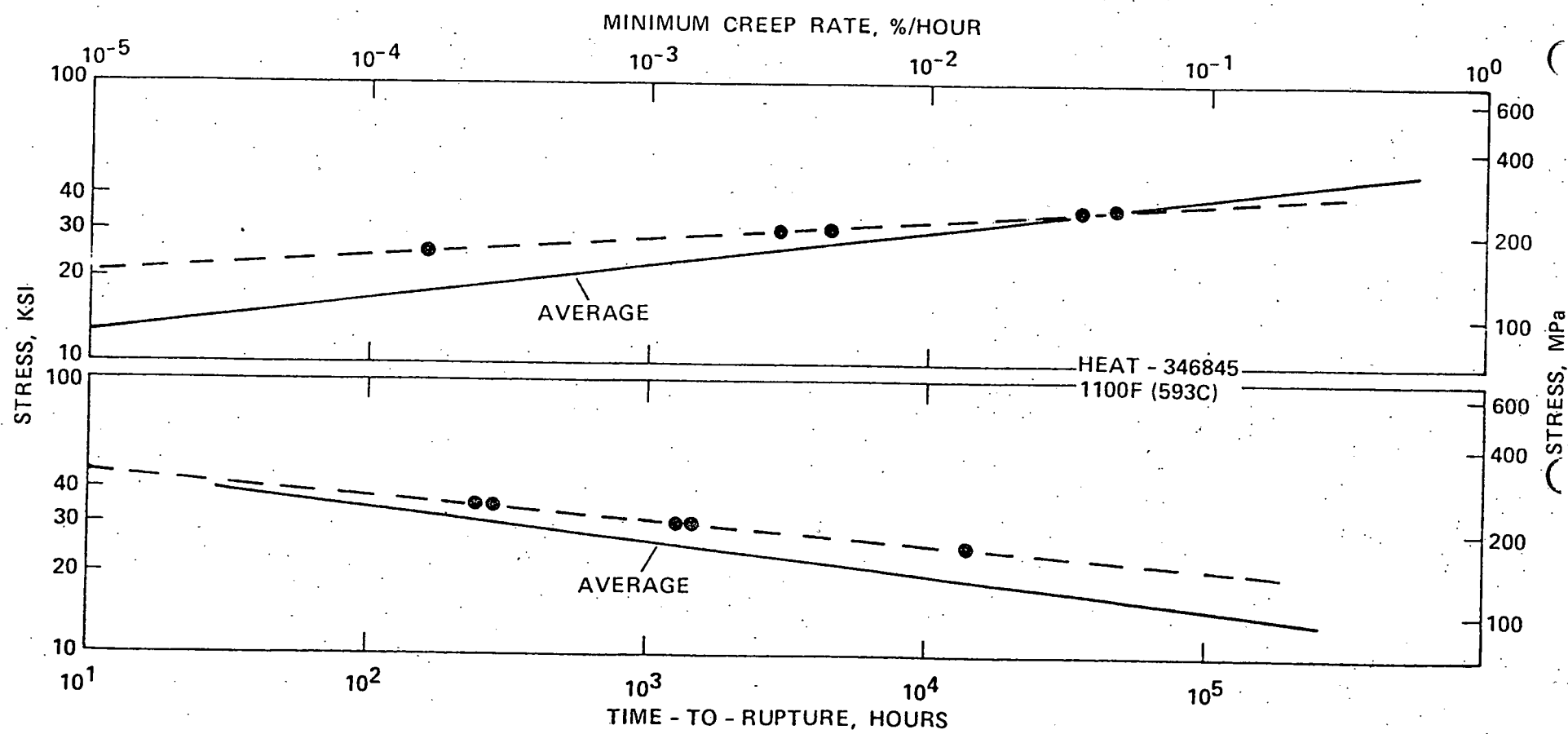
(1) Predictions based on observed creep data.

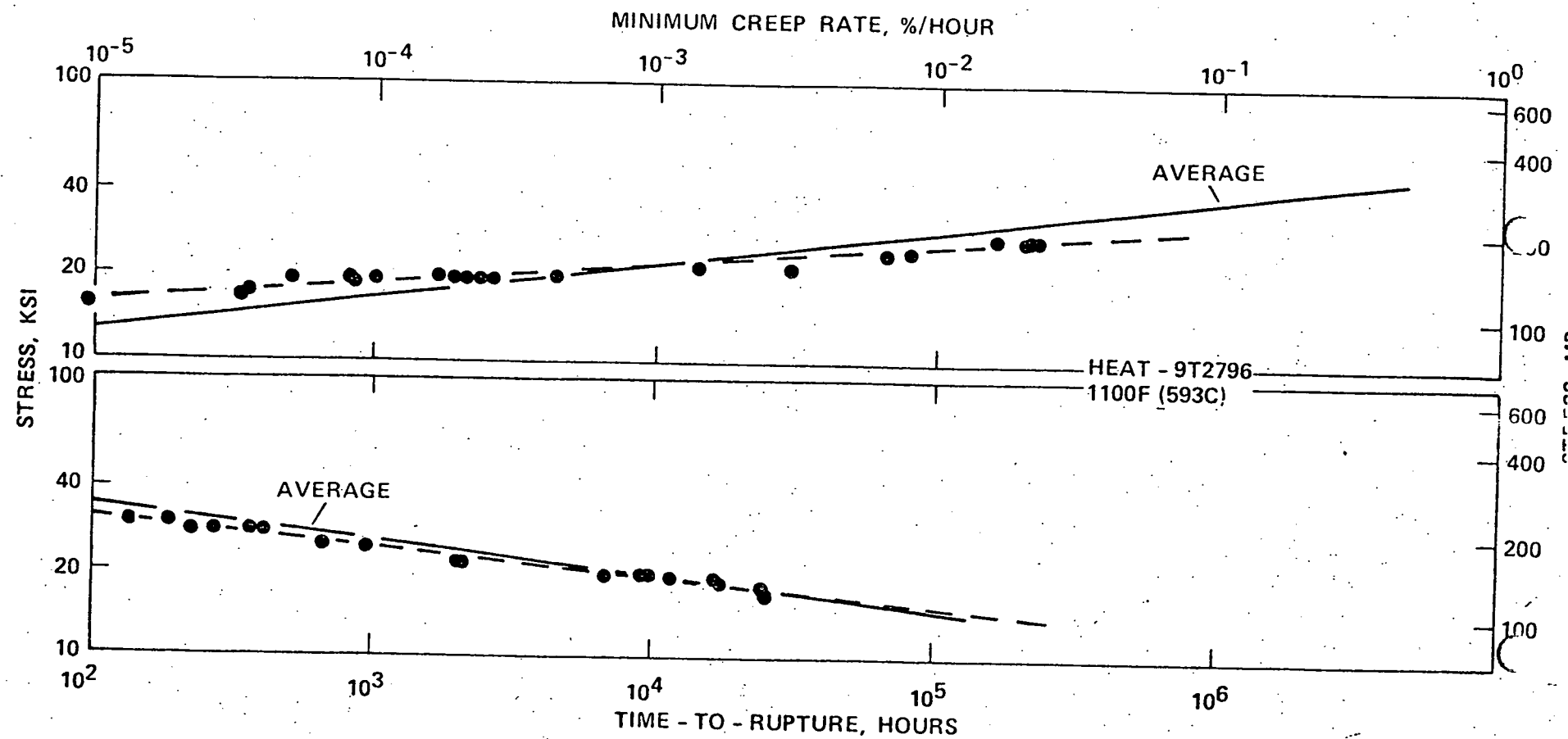
FIGURE TITLES

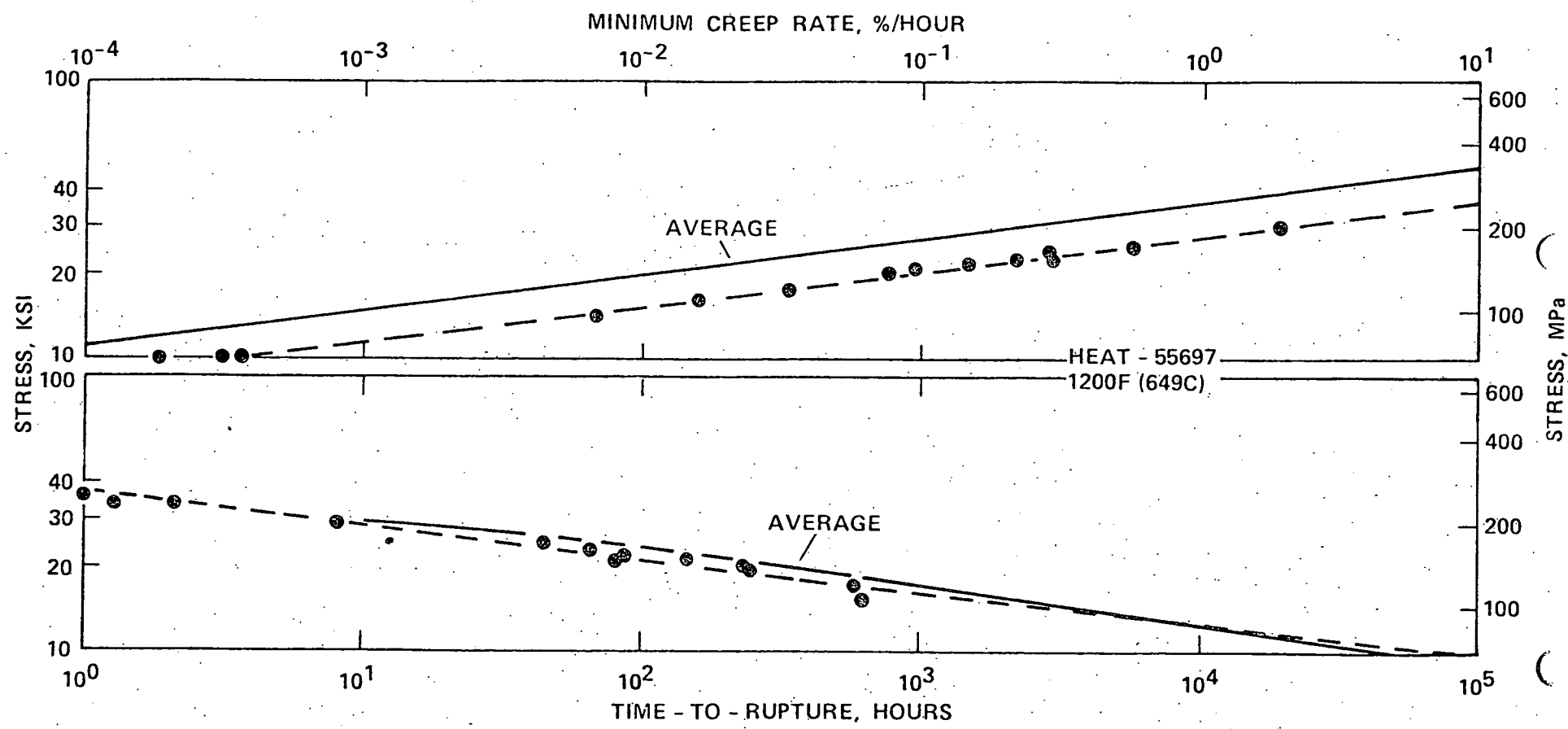
1. Comparison of Observed and Average Minimum Creep Rate Data and Stress Rupture Data. Heat 55697 Tested at 1100F (593C).
2. Comparison of Observed and Average Minimum Creep Rate Data and Stress Rupture Data. Heat 346845 Tested at 1100F (593C).
3. Comparison of Observed and Average Minimum Creep Rate Data and Stress Rupture Data. Heat 9T2796 Tested at 1100F (593C).
4. Comparison of Observed and Average Minimum Creep Rate Data and Stress Rupture Data. Heat 8043813 Tested at 1100F (593C).
5. Comparison of Observed and Average Minimum Creep Rate Data and Stress Rupture Data. Heat 55697 Tested at 1200F (649C).
6. Relationship Between Rupture Strength (10^3 Hours) and Creep Strength ($1/10^2$ Hours).
7. Relationship Between Rupture Strength (10^4 Hours) and Creep Strength ($1/10^3$ Hours).
8. Relationship Between Rupture Strength (10^5 Hours) and Creep Strength ($1/10^4$ Hours).
9. Stress Range as a Function of Hold-Time. Determined Near Half-Life During Hold-Time Fatigue Tests. Tested at 1100F (593C) with a Strain Range of 1%.
10. Fatigue Life Reduction Factor as a Function of Hold-Time. No Explicit Factor of Safety. Heat 55697 Tested at 1200F (649C) and a Strain Range of 1/2%.
11. Fatigue Life Reduction Factor as a Function of Hold-Time. Factor of 1/0.9 on Stress. Heat 55697 Tested at 1200F (649C) and a Strain Range of 1/2%.
12. Fatigue Life Reduction Factor as a Function of Hold-Time. Full Code-Intended Factors of Safety. Heat 55697 Tested at 1200F (649C) and a Strain Range of 1/2%.
13. Fatigue Life Reduction Factor as a Function of Hold-Time. No Explicit Factor of Safety. Heat 346845 Tested at 1100F (593C) and a Strain Range of 1%.
14. Fatigue Life Reduction Factor as a Function of Hold-Time. Factor of 1/0.9 on Stress. Heat 346845 Tested at 1100F (593C) and a Strain range of 1%.
15. Fatigue Life Reduction Factor as a Function of Hold-Time. Full Code-Intended Factors of Safety. Heat 346845 Tested at 1100F (593C) and a Strain Range of 1%.

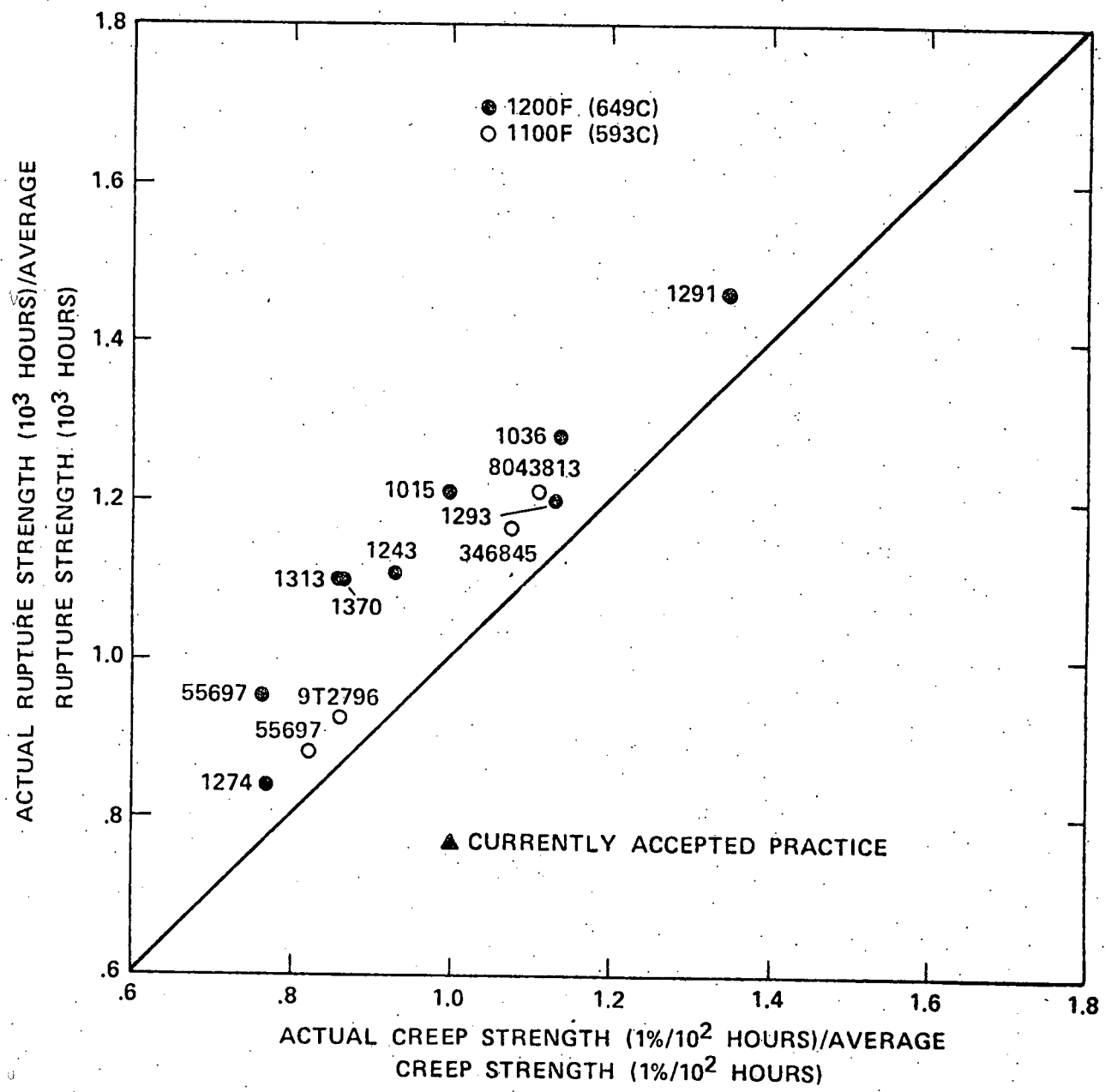
16. Fatigue Life Reduction Factor as a Function of Hold-Time. No Explicit Factor of Safety. Heat 9T2796 Tested at 1100F (593C) and a Strain Range of 1%.
17. Fatigue Life Reduction Factor as a Function of Hold-Time. Factor of 1/0.9 on Stress. Heat 9T2796 Tested at 1100F (593C) and a Strain Range of 1%.
18. Fatigue Life Reduction Factor as a Function of Hold-Time. Full Code-Intended Factors of Safety. Heat 9T2796 Tested at 1100F (593C) and a Strain Range of 1%.
19. Fatigue Life Reduction Factor as a Function of Hold-Time. No Explicit Factor of Safety. Heat 8043813 Tested at 1100F (593C) and a Strain Range of 1%.
20. Fatigue Life Reduction Factor as a Function of Hold-Time. Factor of 1/0.9 on Stress. Heat 8043813 Tested at 1100F (593C) and a Strain Range of 1%.
21. Fatigue Life Reduction Factor as a Function of Hold-Time. Full Code-Intended Factors of Safety. Heat 8043813 Tested at 1100F (593C) and a Strain Range of 1%.
22. Effect of Code-Intended Factors of Safety on Predicted Fatigue Life Reduction Factors at 1100F (593C) and a Strain Range of 1%.
23. Comparison of Predicted and Observed Stress Relaxation During Hold-Time Fatigue Testing of Heat 55697. Tested at 1200F (649C) with a Strain Range of 1/2% and a Hold-Time of 60 Minutes.
24. Comparison of Predicted and Observed Stress Relaxation During Hold-Time Fatigue Testing of Heat 346845. Tested at 1100F (593C) with a Strain Range of 1% and a Hold-Time of 60 Minutes.
25. Comparison of Predicted and Observed Hold-Time Fatigue Lives. Life Predictions Based on Observed Stress Relaxation History (Near Half-Life) and Observed Rupture Strengths. No explicit Factors of Safety.
26. Comparison of Predicted and Observed Hold-Time Fatigue Lives. Life Predictions Based on Currently Accepted Practice. No Explicit Factors of Safety.
27. Comparison of Predicted and Observed Hold-Time Fatigue Lives. Life Predictions Based on Observed Creep and Rupture Strengths and Observed Stress Range. No Explicit Factors of Safety.
28. Comparison of Predicted and Observed Hold-Time Fatigue Lives. Life Predictions Based on Observed Creep and Rupture Strengths and the NSMH Estimated Stress Range. No Explicit Factors of Safety.
29. Comparison of Predicted and Observed Hold-Time Fatigue Lives. Life Predictions Based on Consistent Creep and Rupture Strengths for a Minimum Strength Heat. No Explicit Factors of Safety.

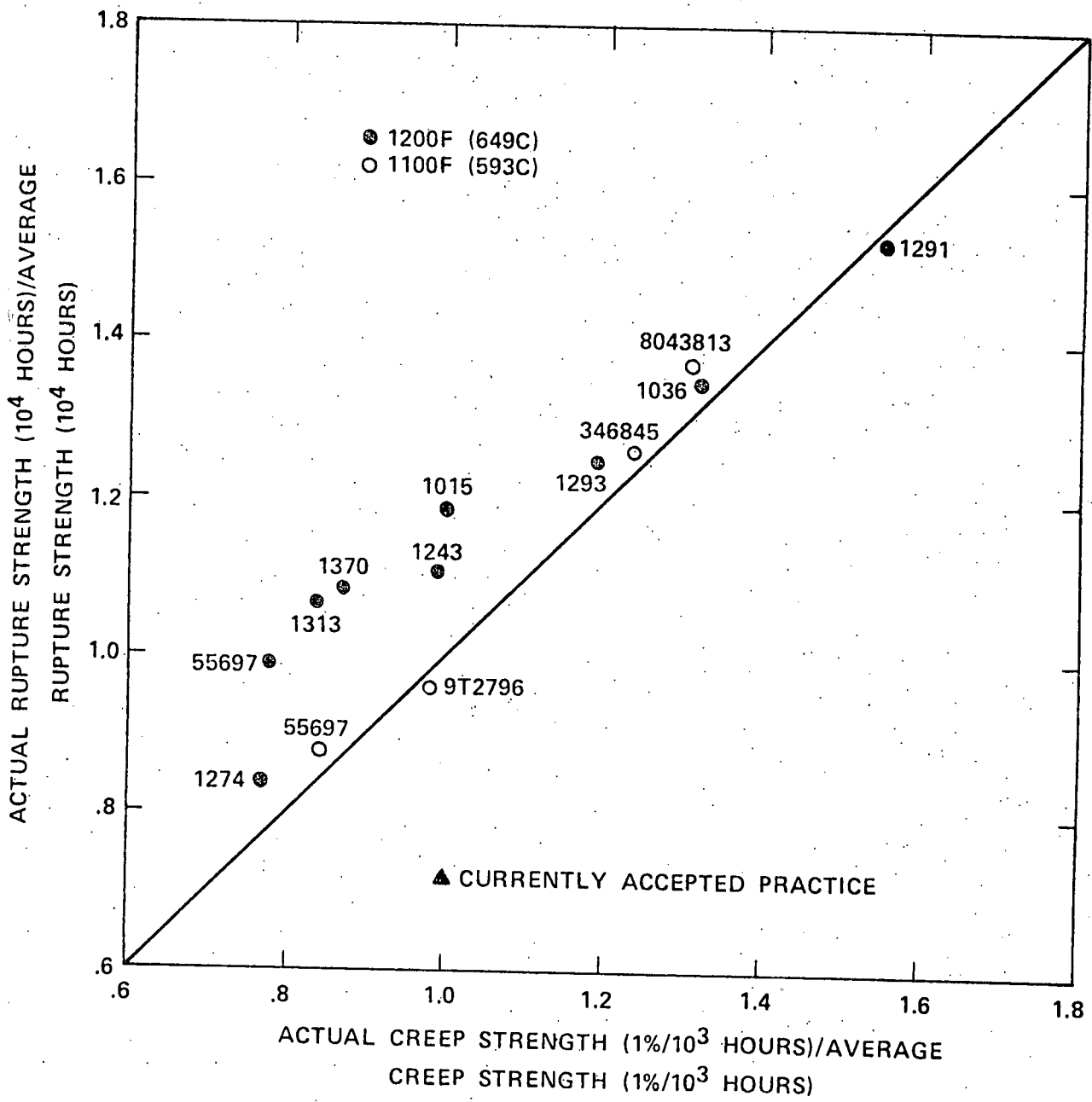


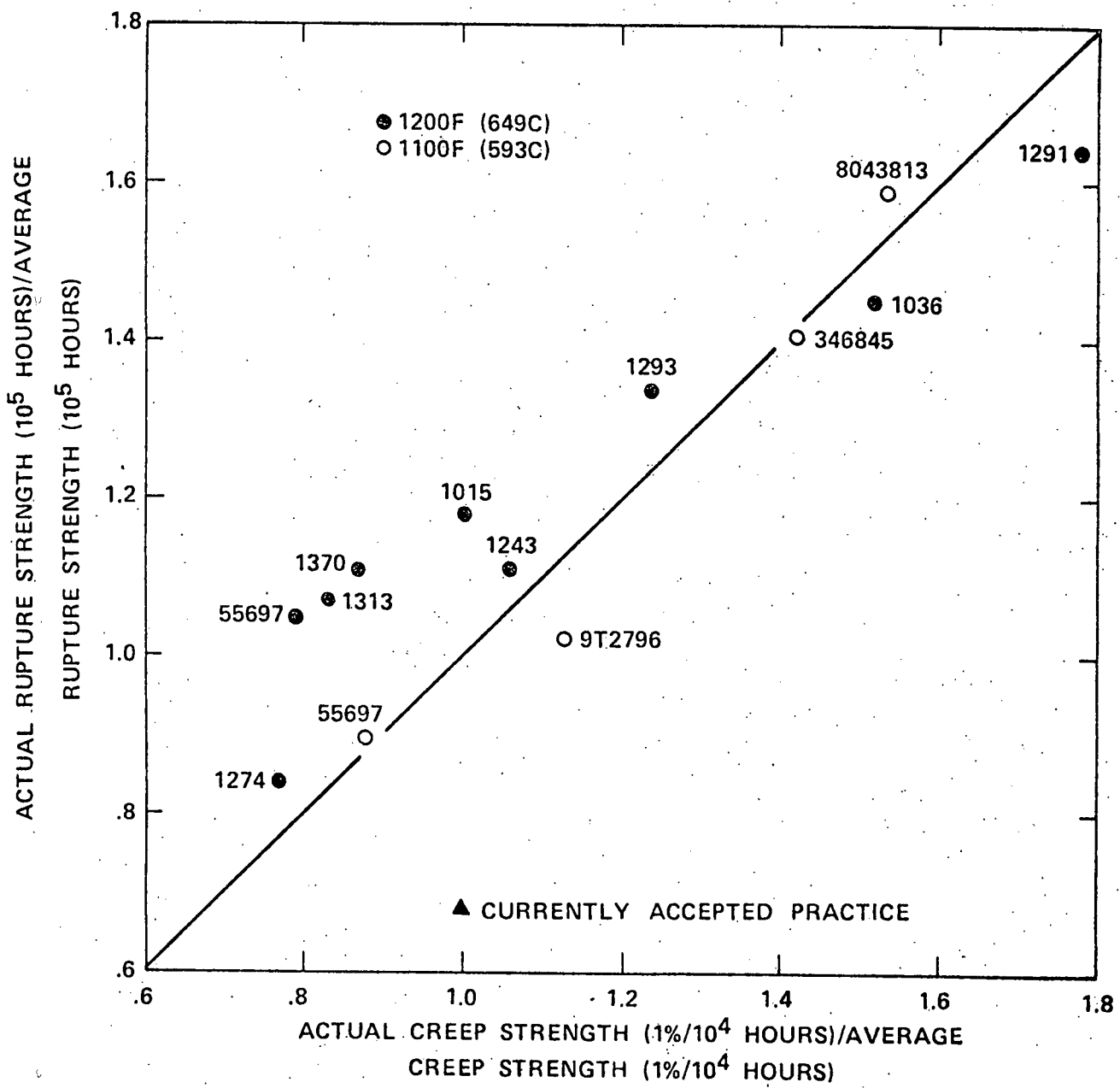


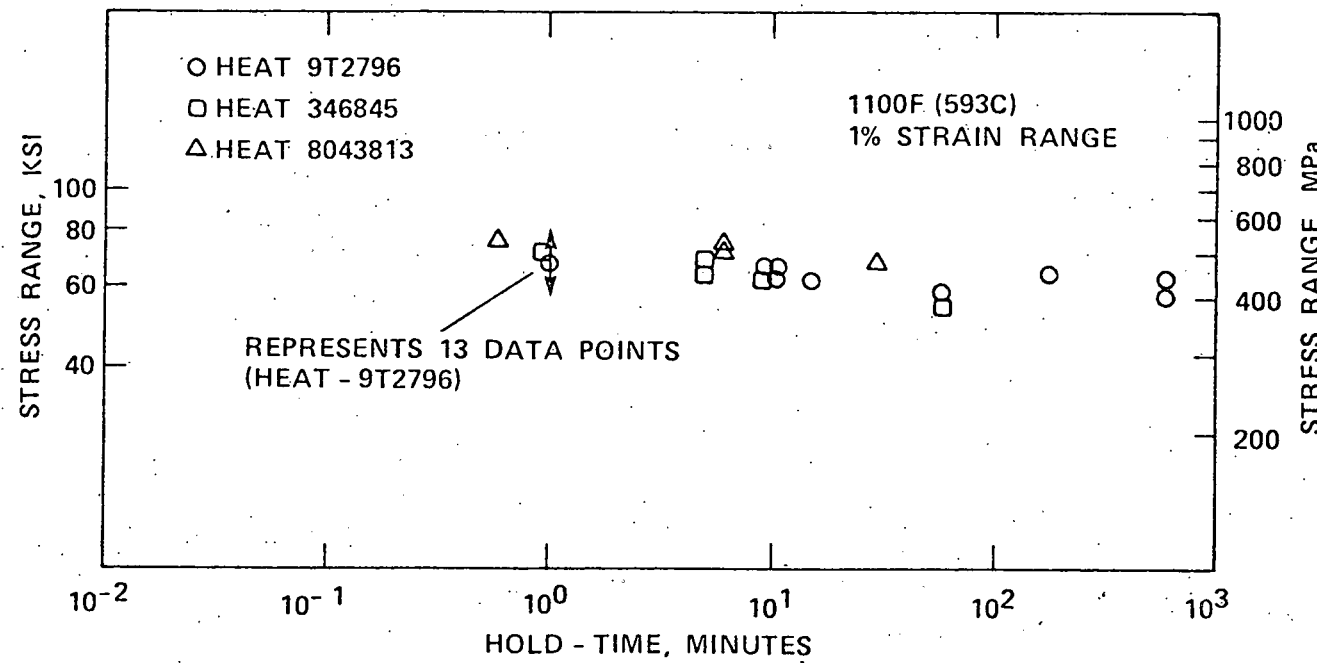


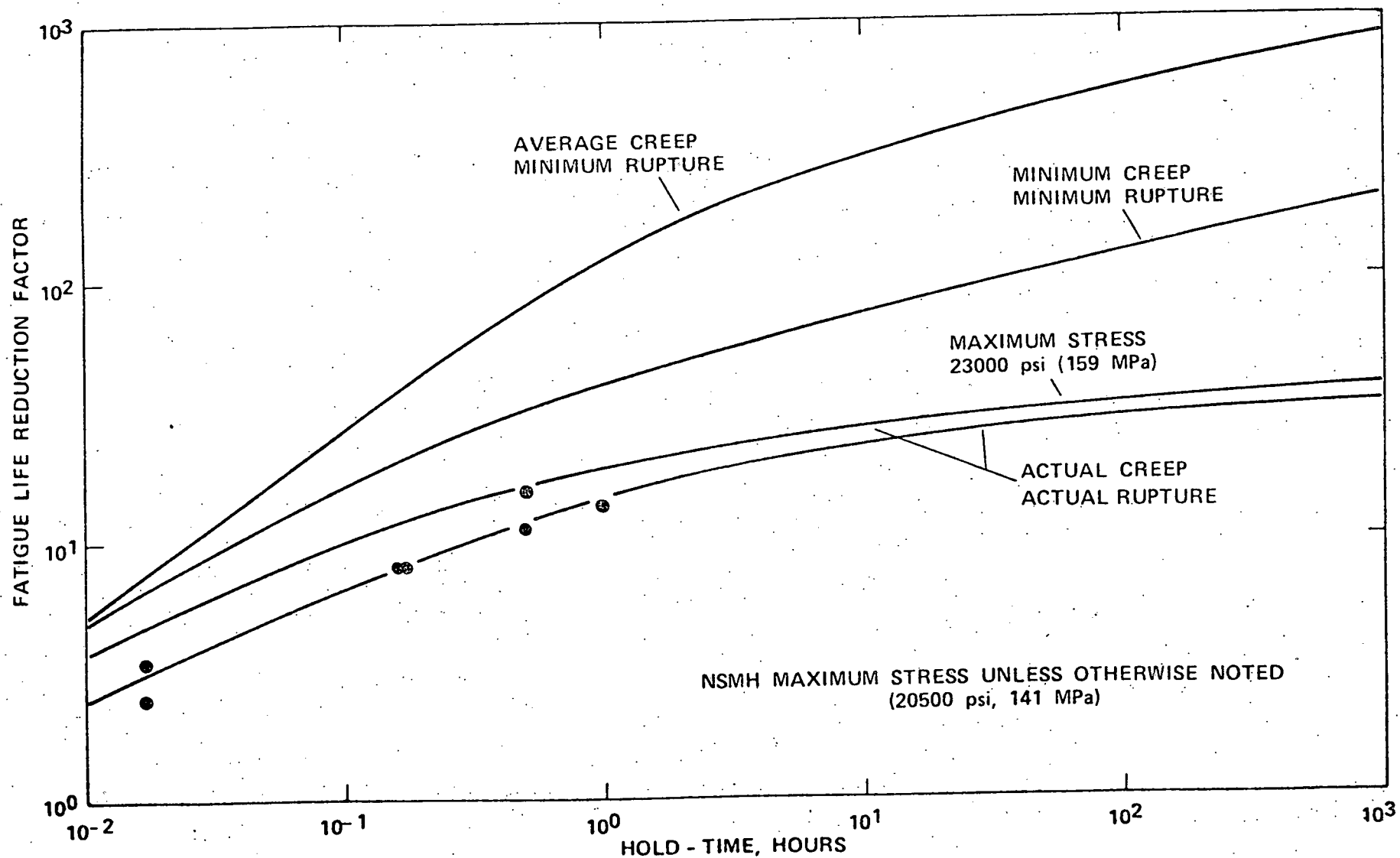


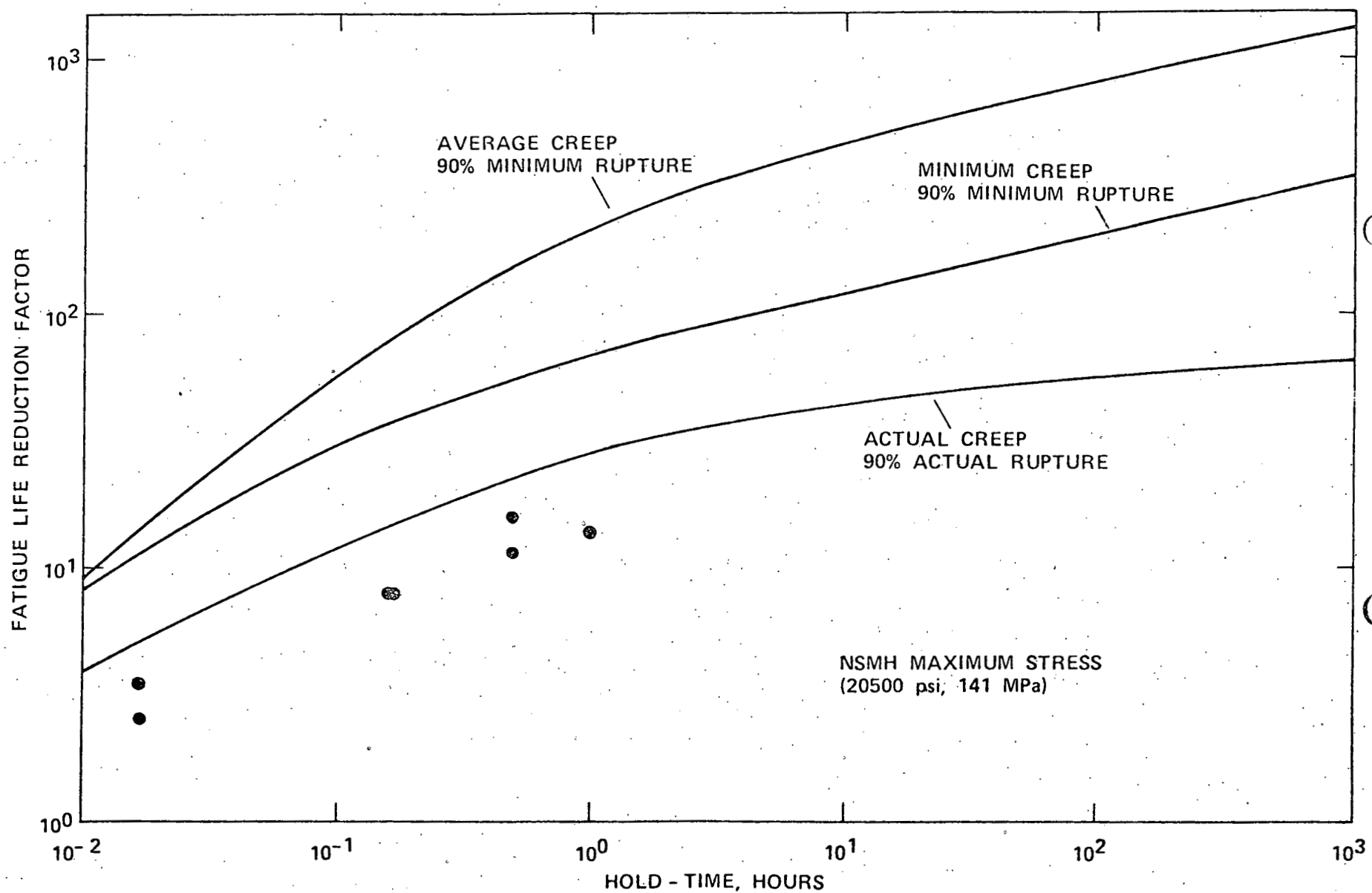


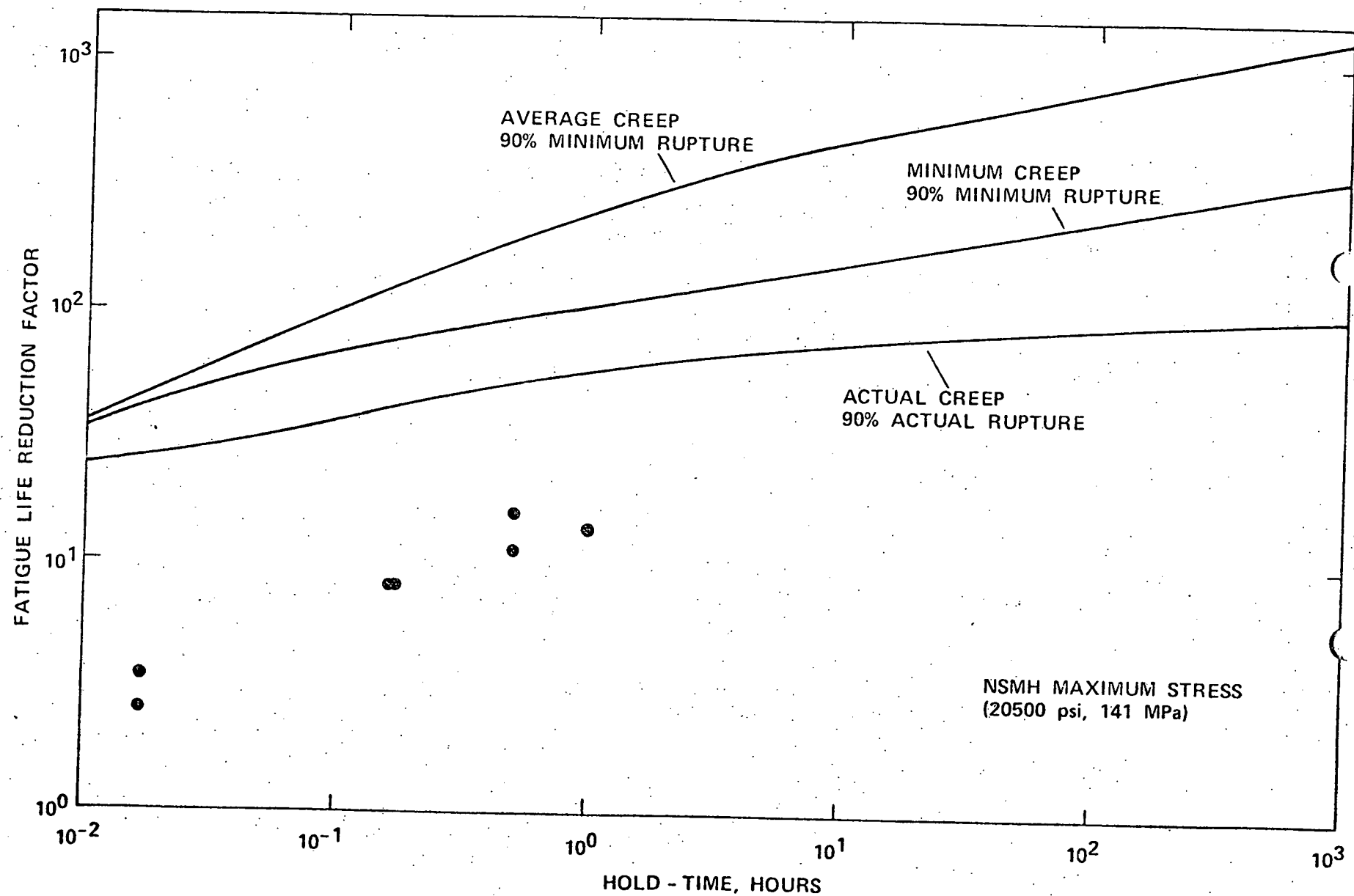


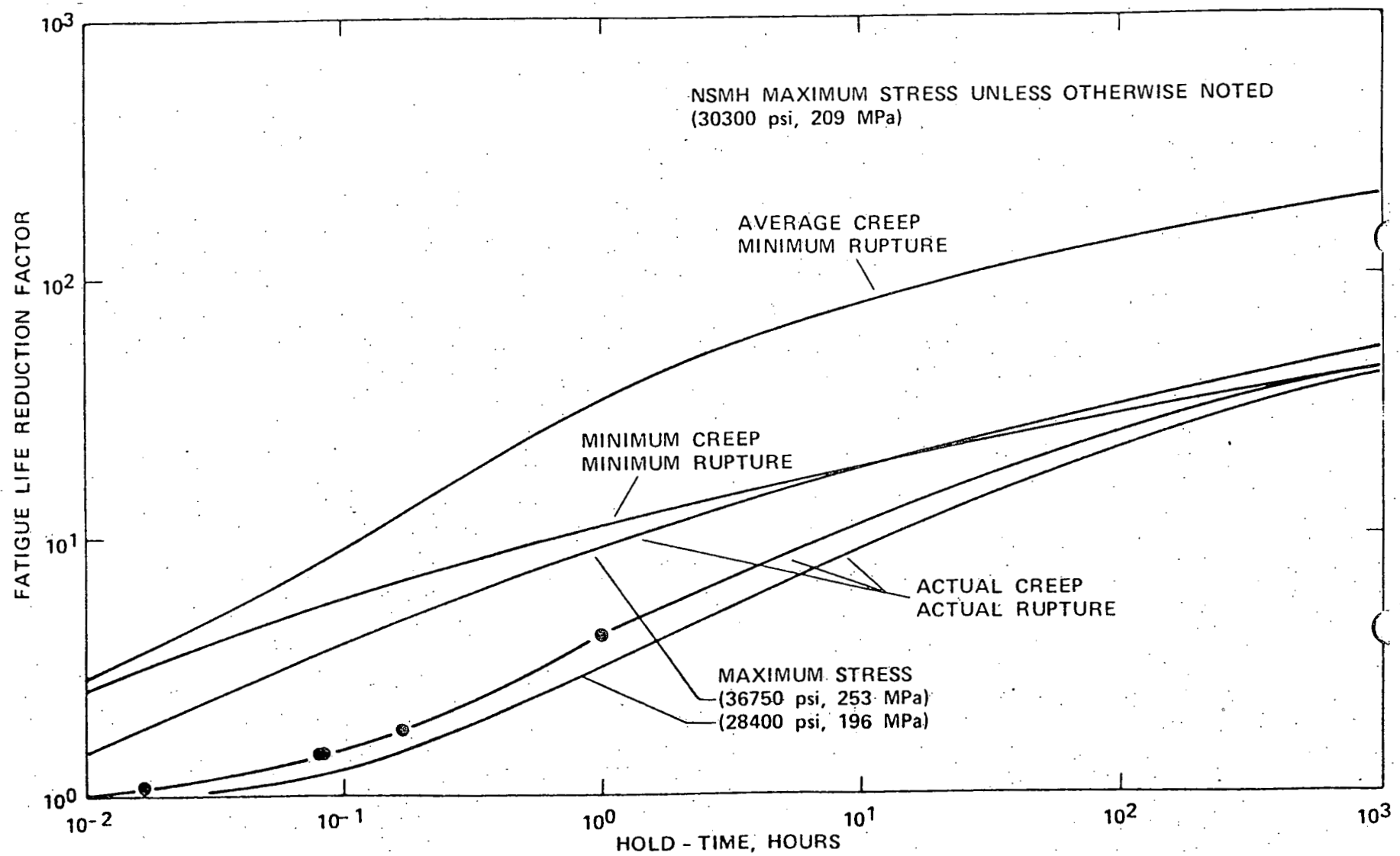


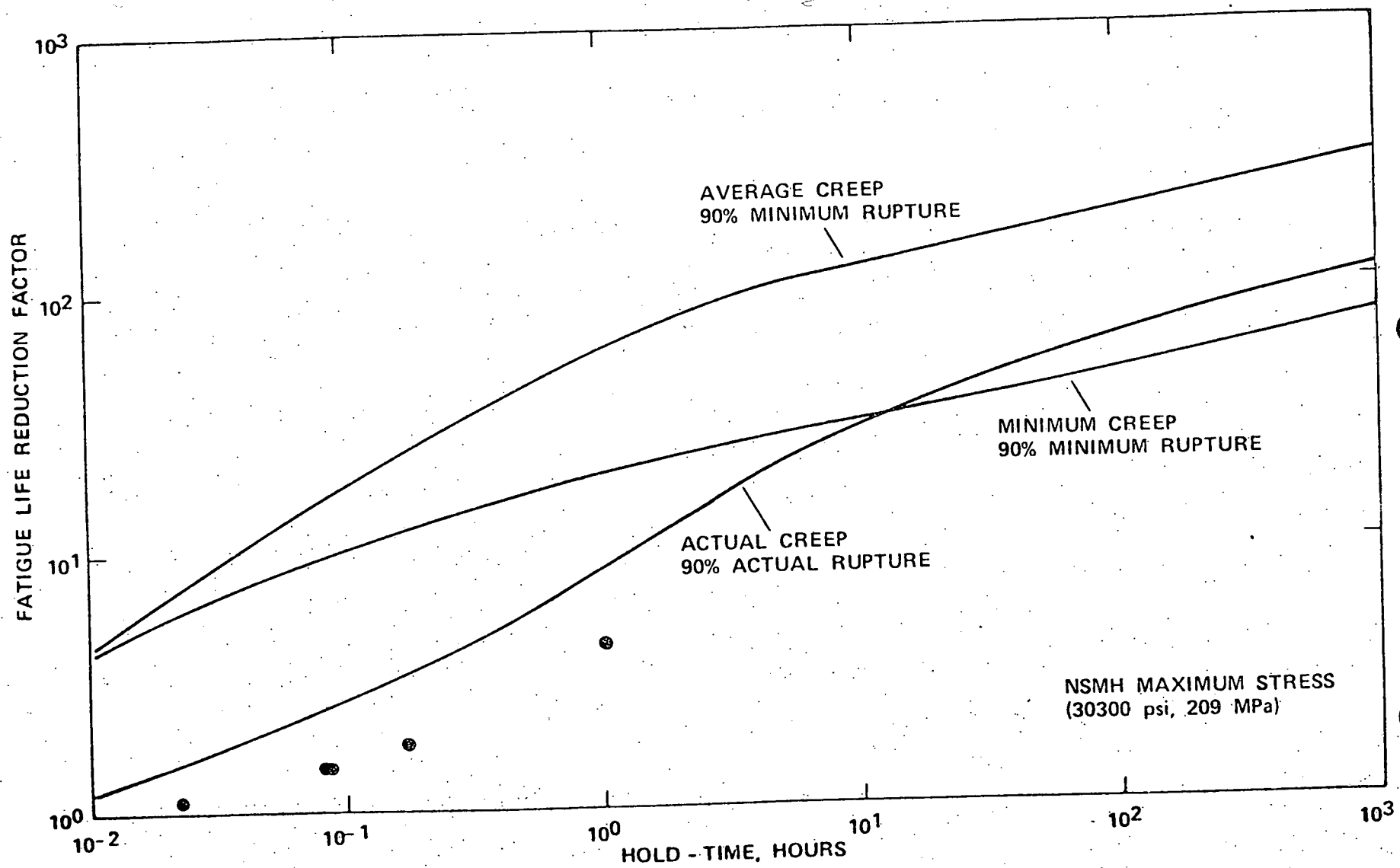


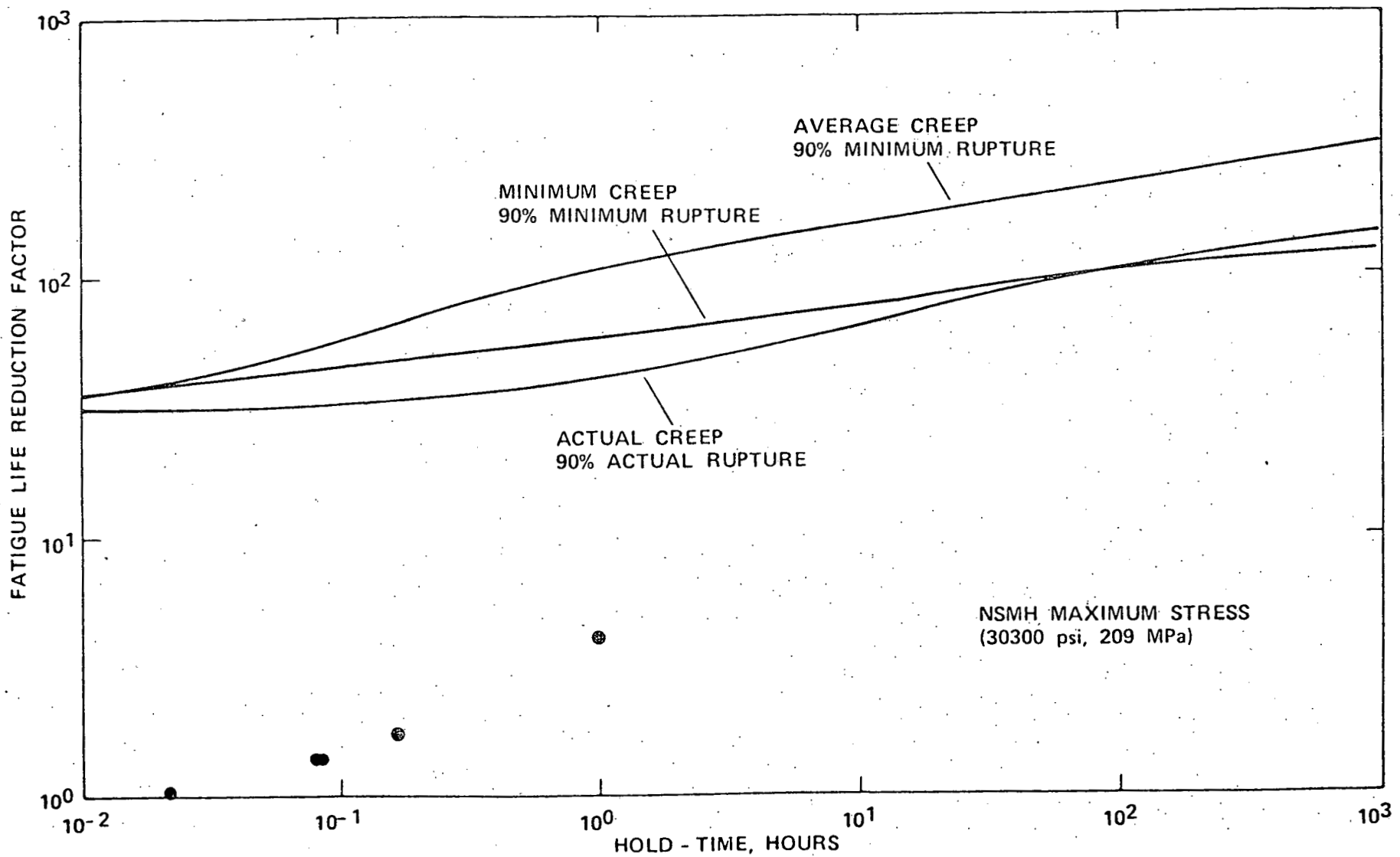


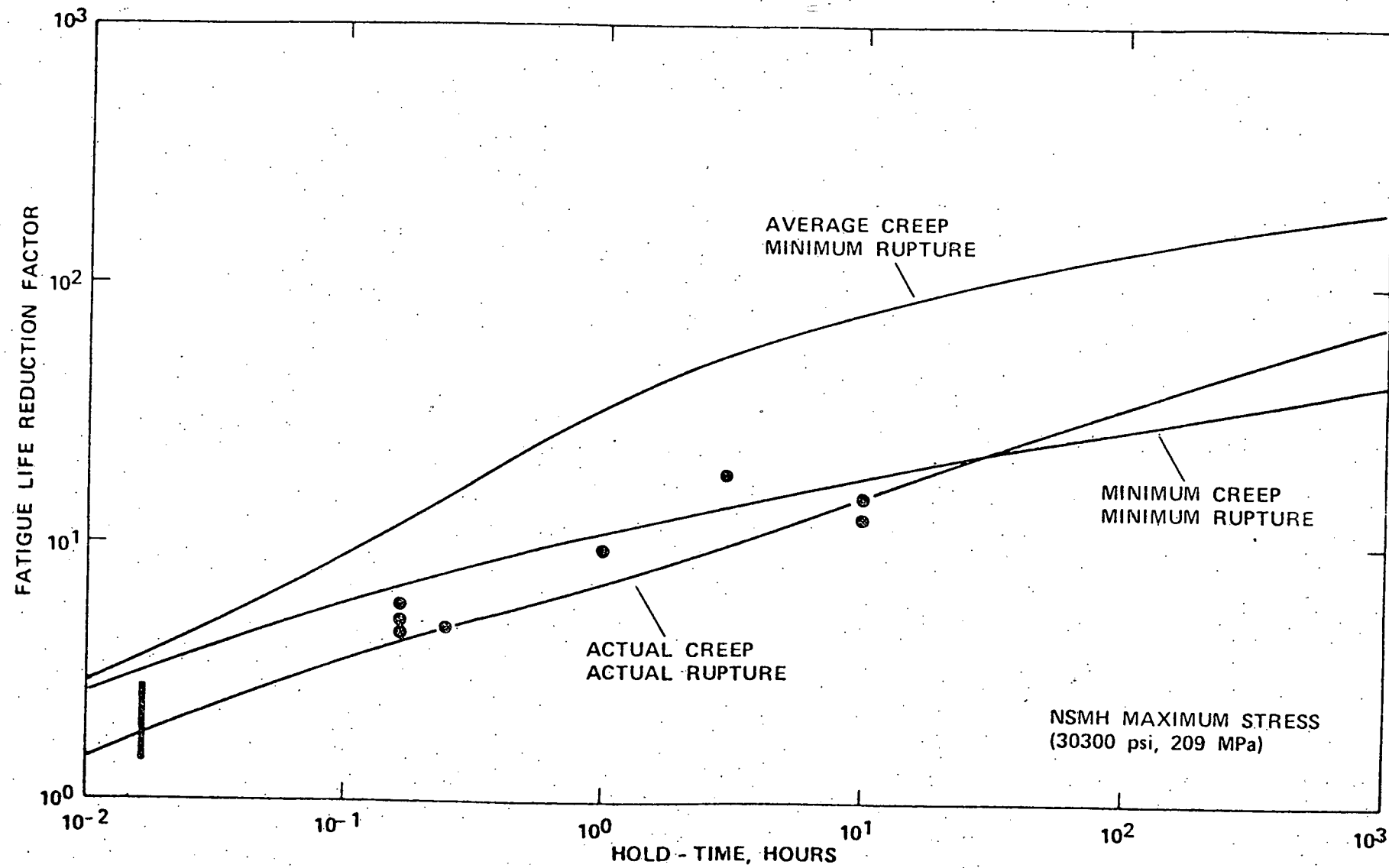


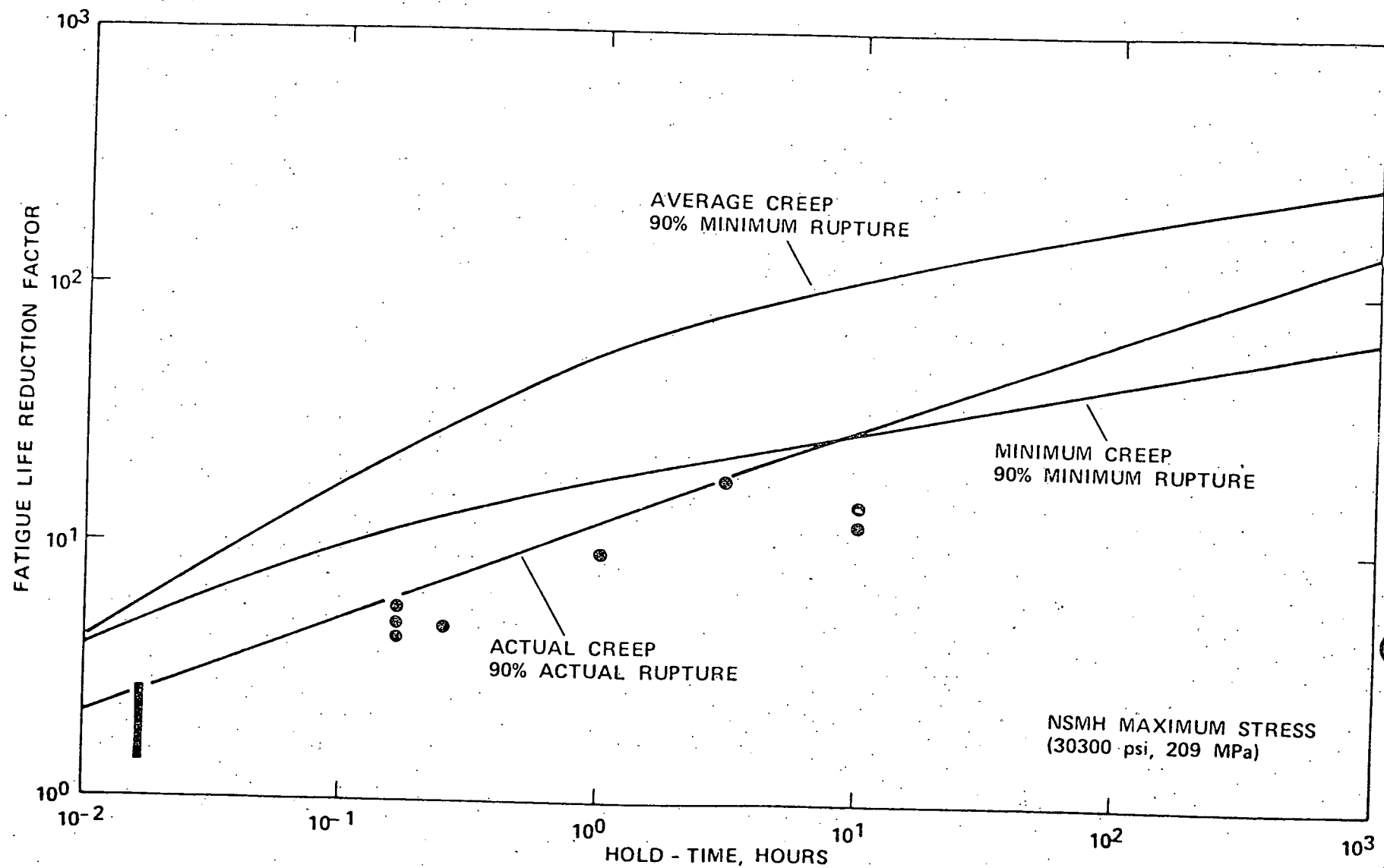


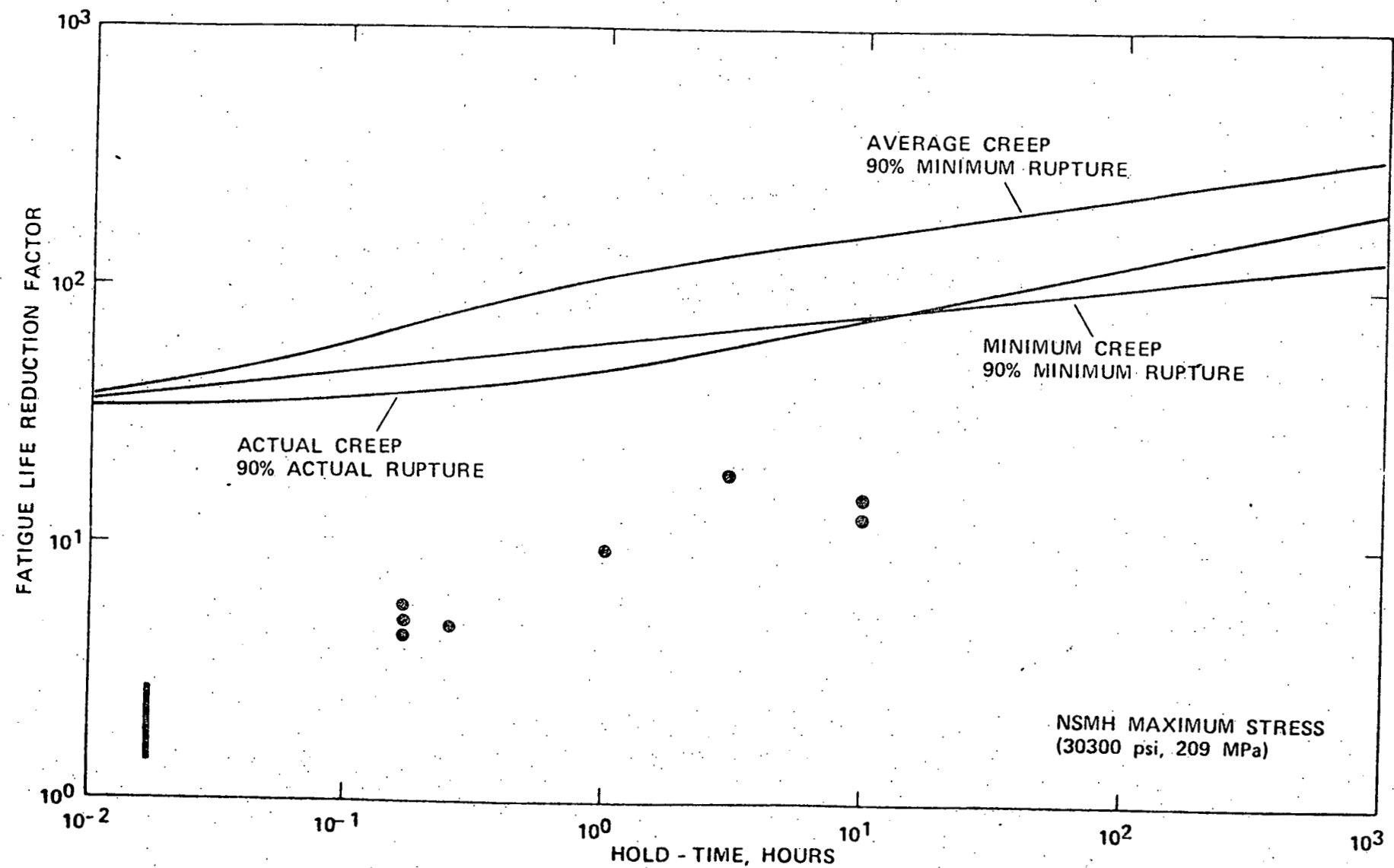












10³

FATIGUE LIFE REDUCTION FACTOR

10²

10¹

10⁰

AVERAGE CREEP
MINIMUM RUPTURE

MINIMUM CREEP
MINIMUM RUPTURE

ACTUAL CREEP
ACTUAL RUPTURE

MAXIMUM STRESS
(39100 psi, 270 MPa)
(35200 psi, 243 MPa)

NSMH MAXIMUM STRESS UNLESS OTHERWISE NOTED
(30300 psi, 209 MPa)

10⁻²

10⁻¹

10⁰

10¹

10²

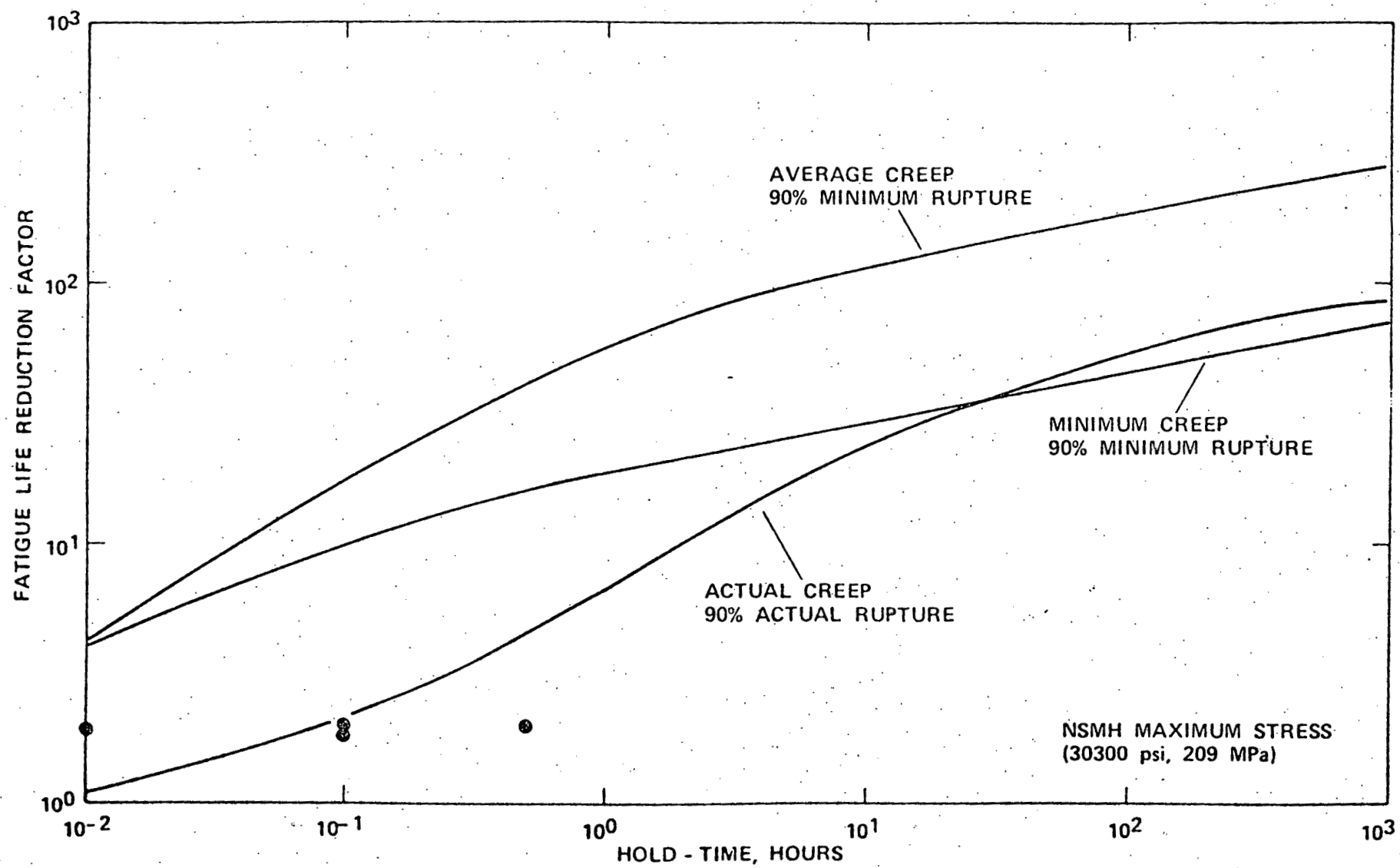
10³

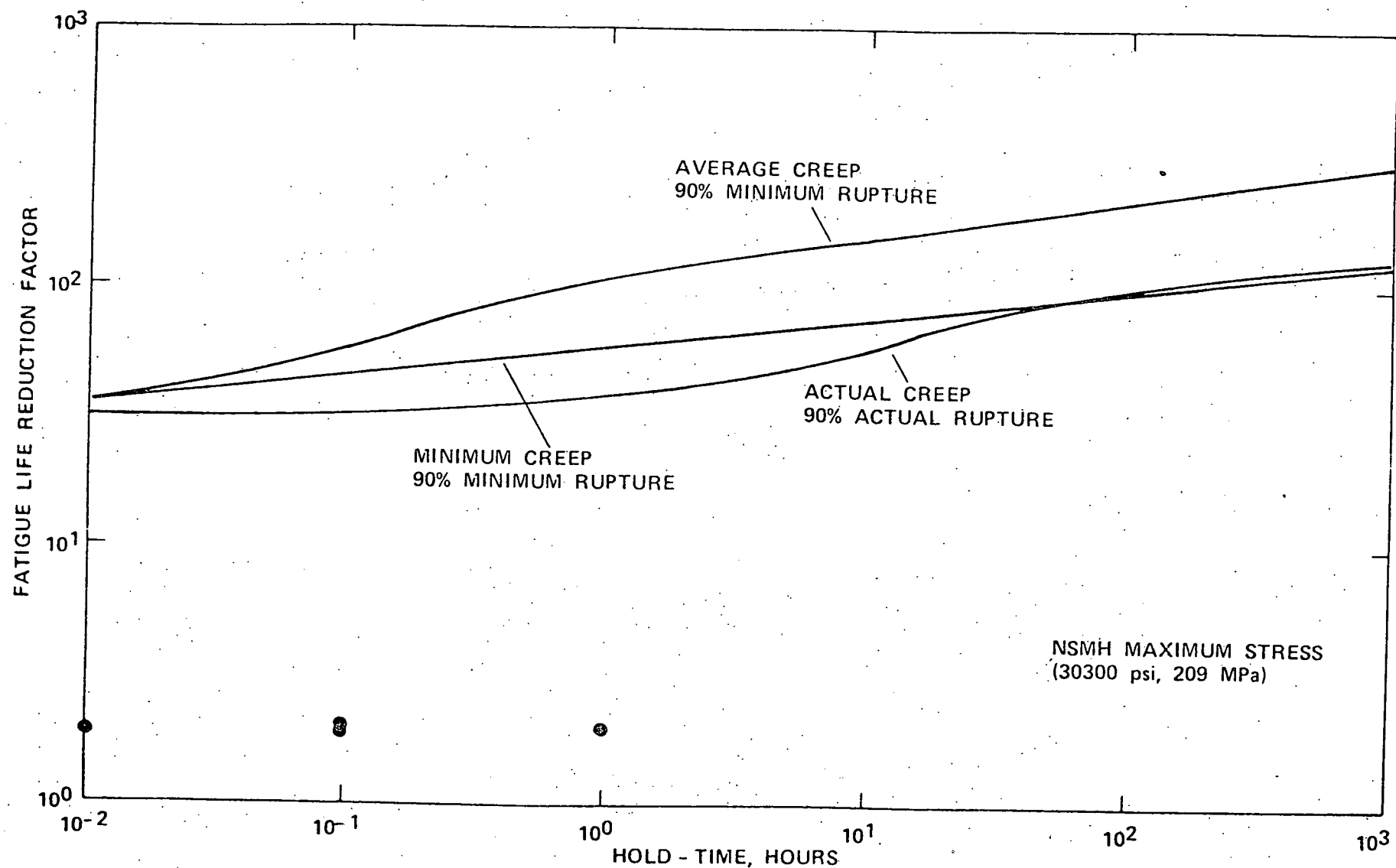
HOLD - TIME, HOURS

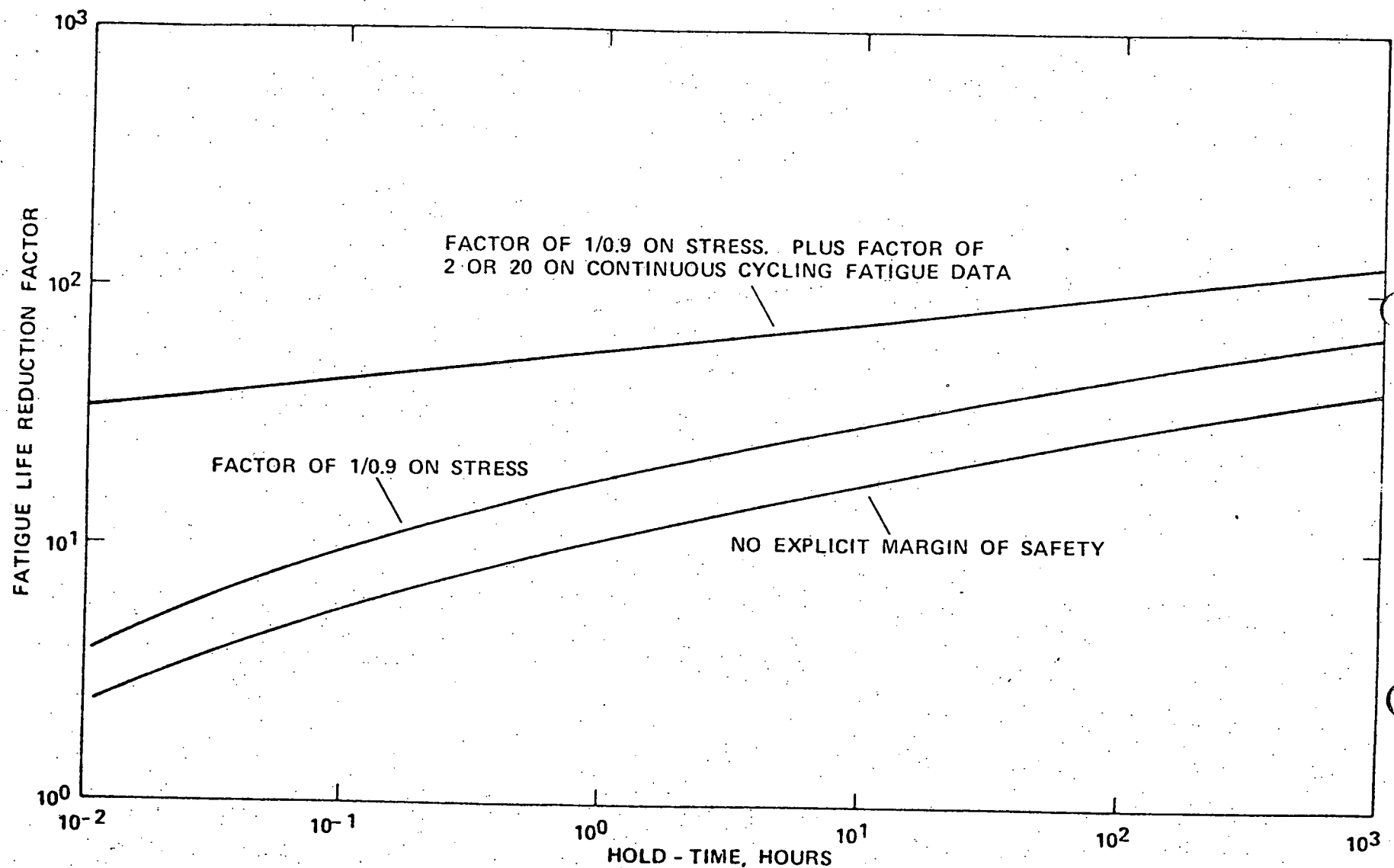
•

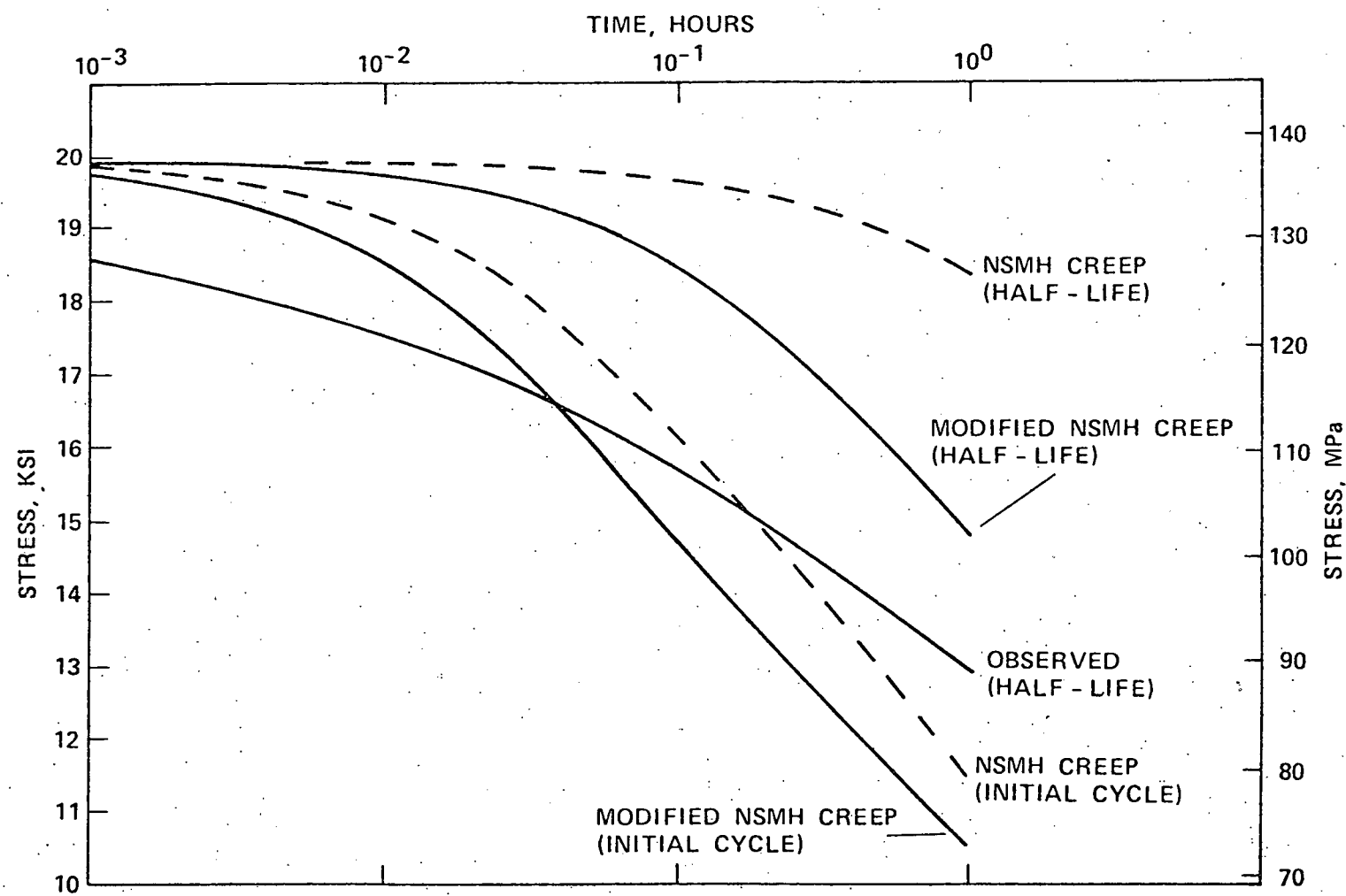
•

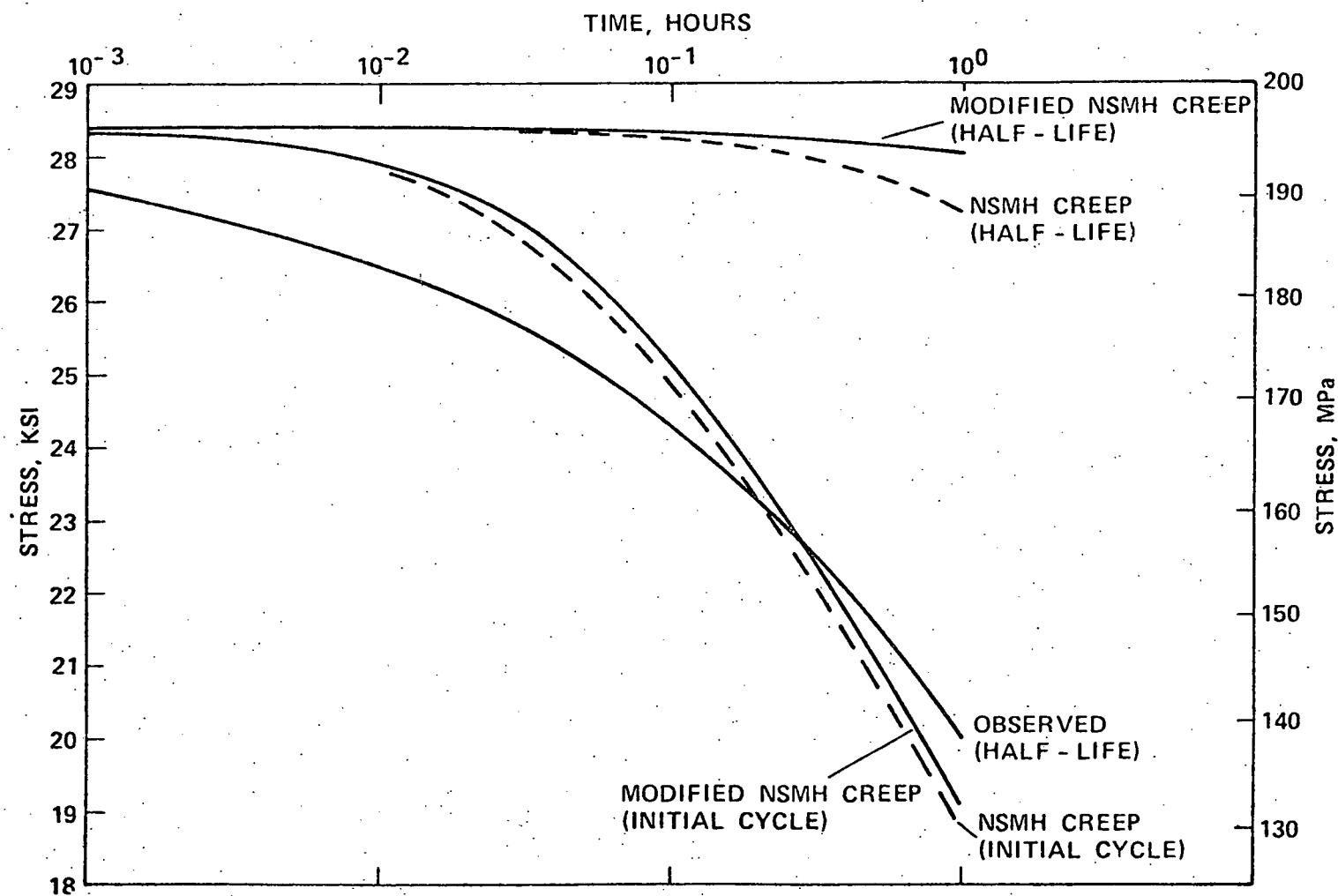
•

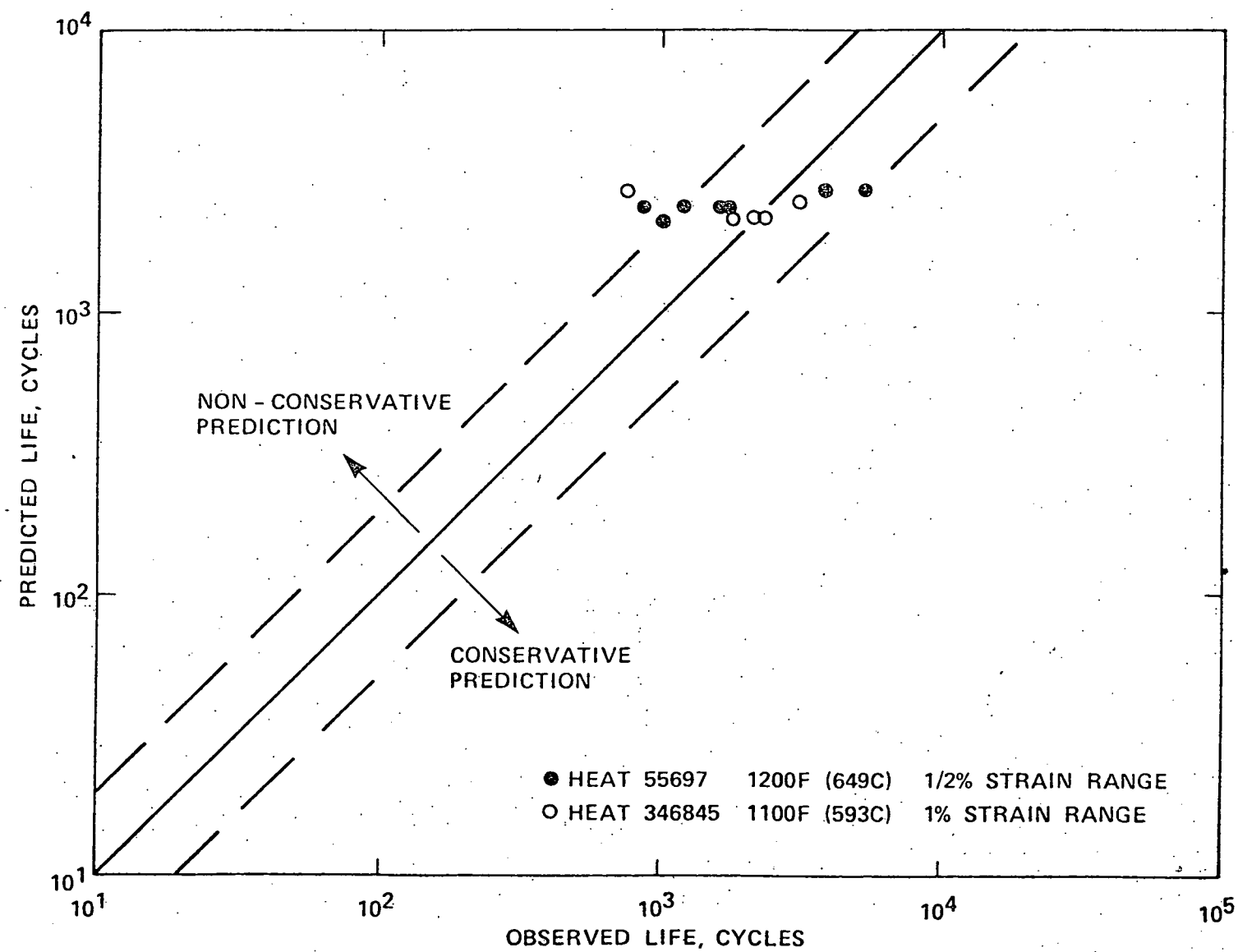


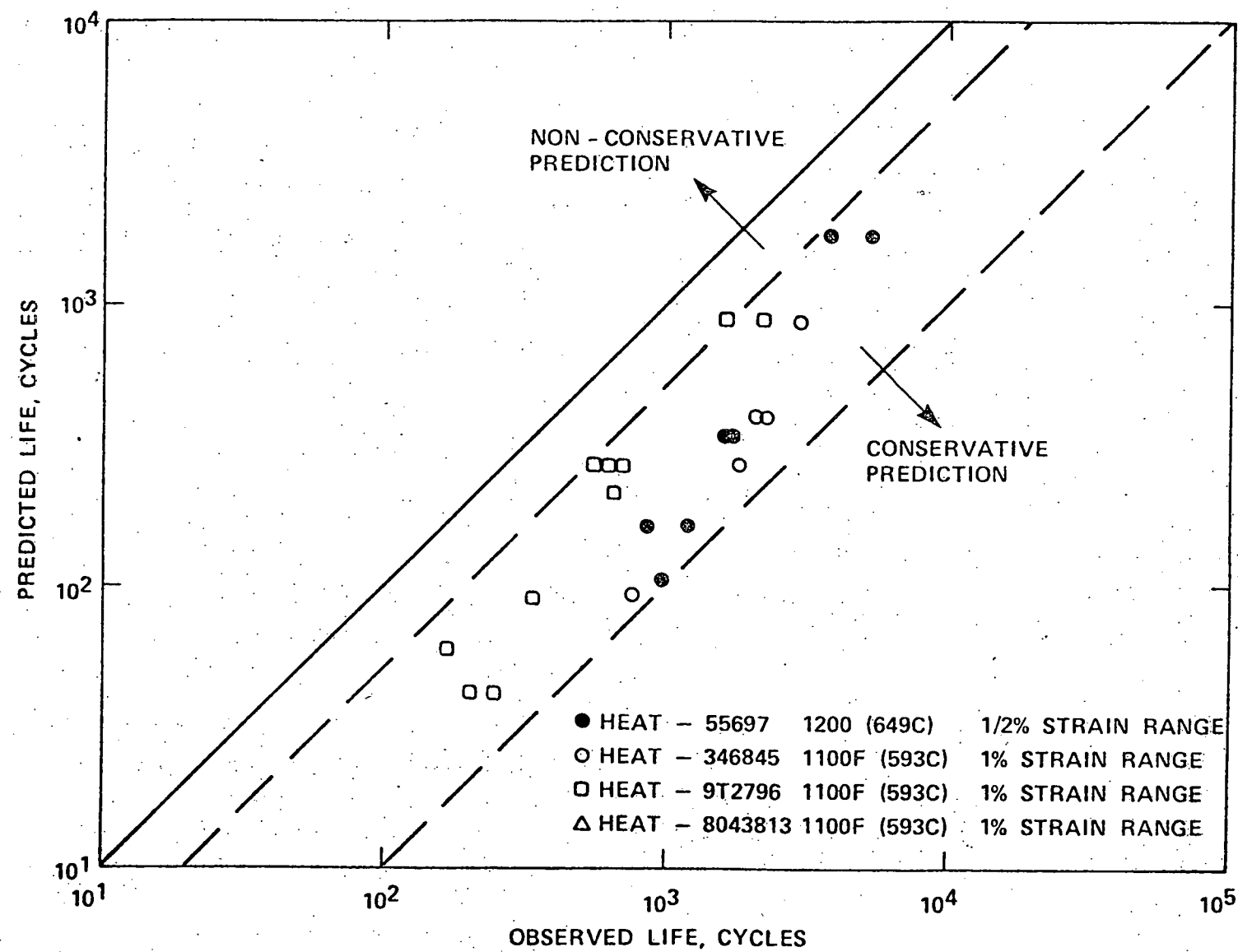


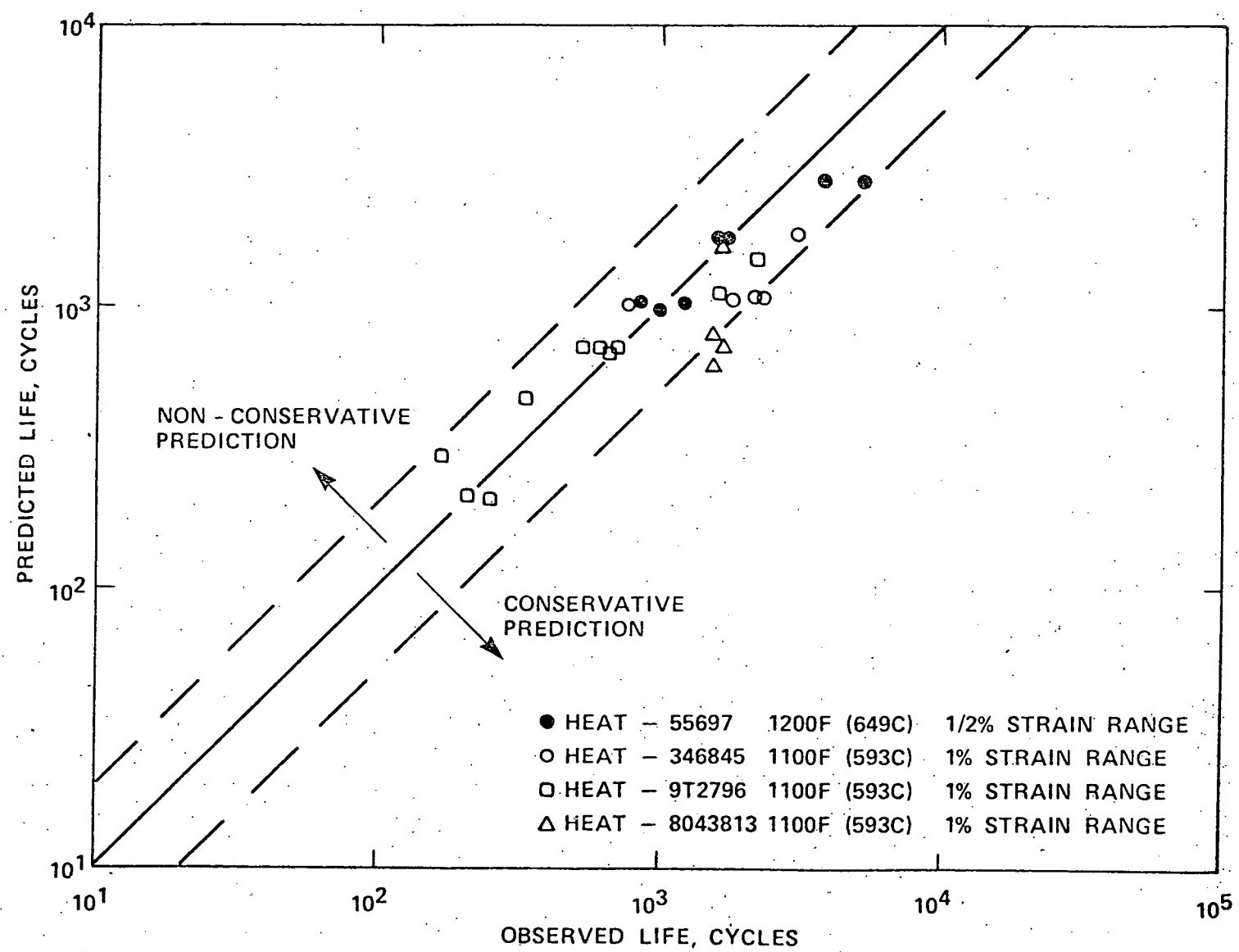


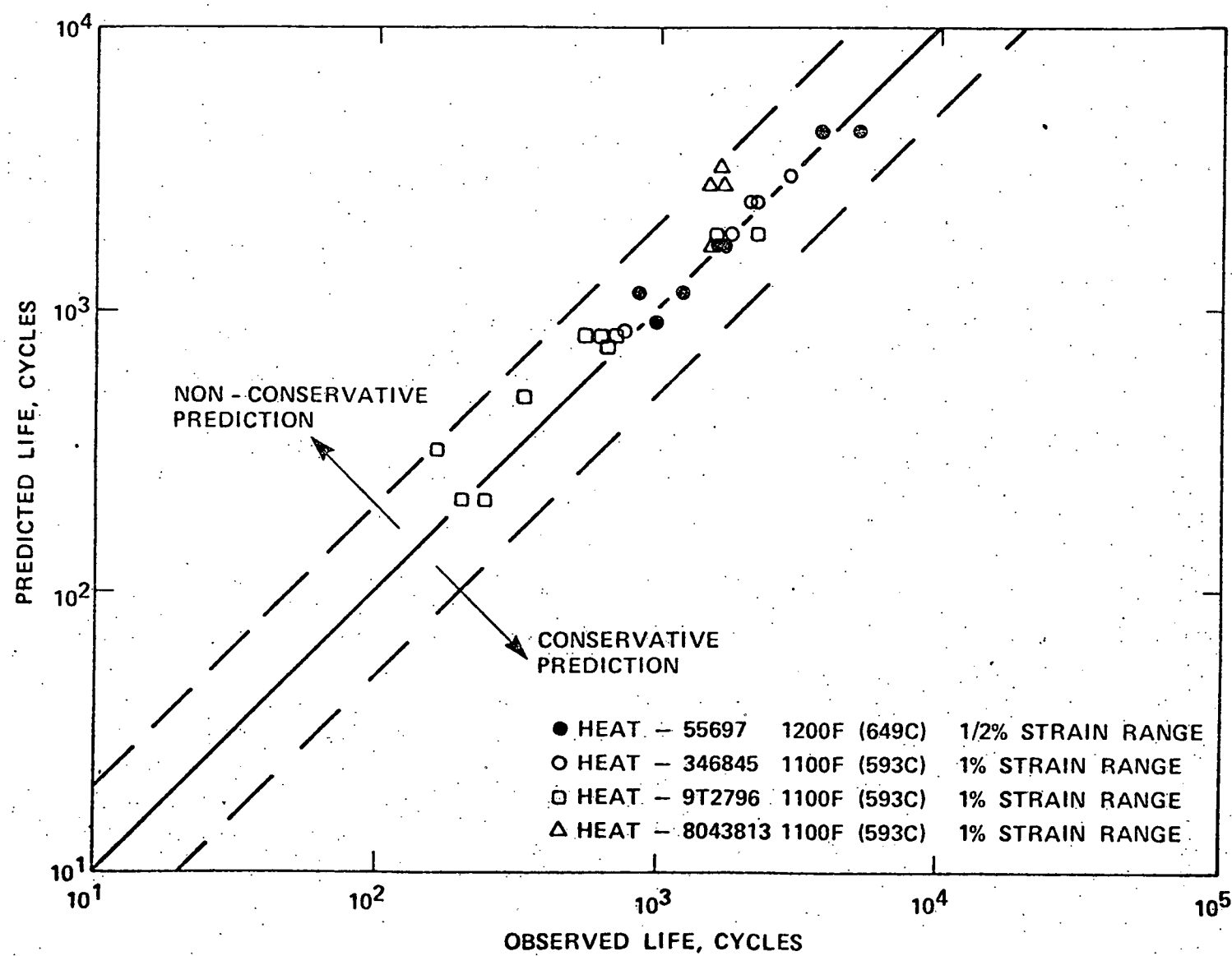


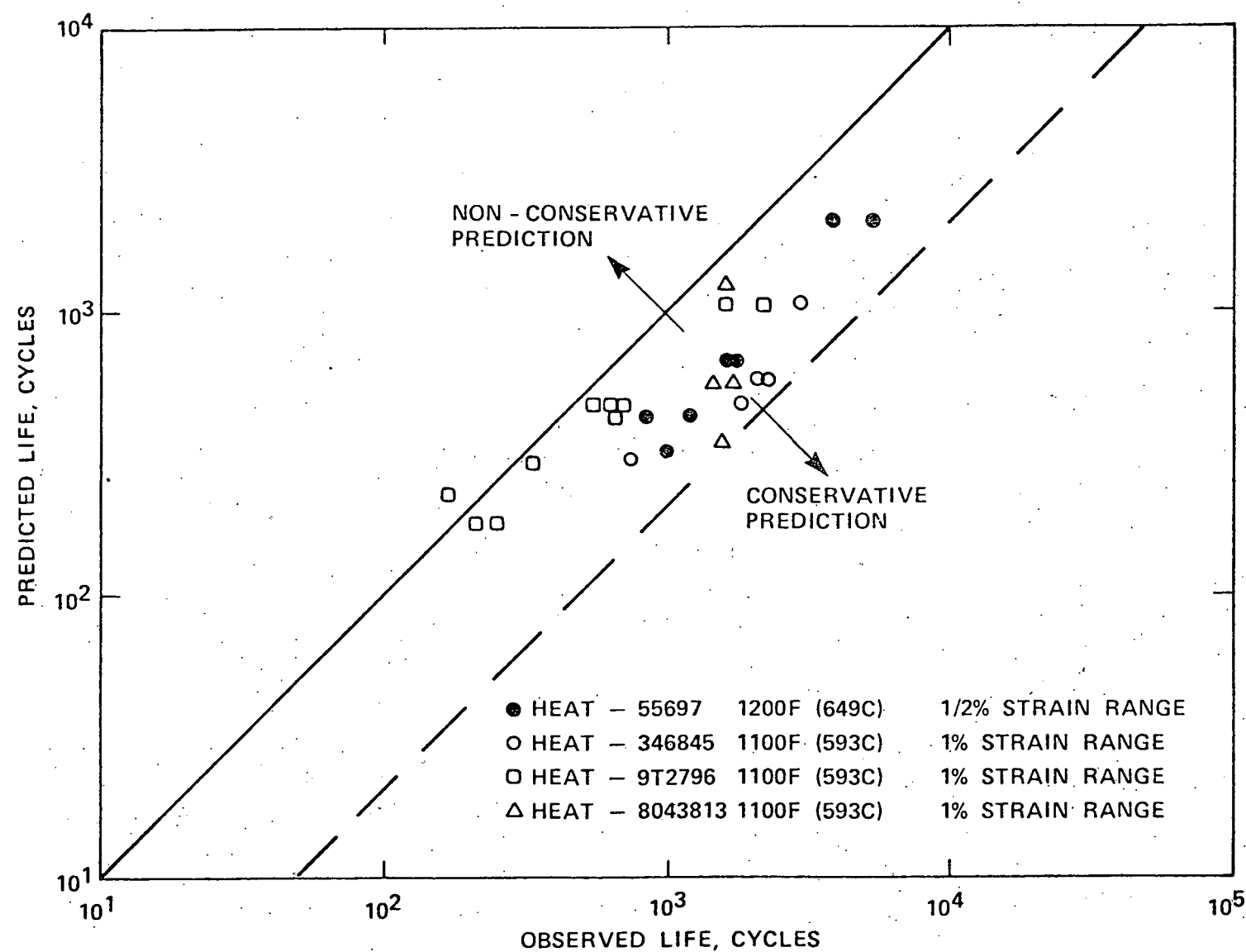












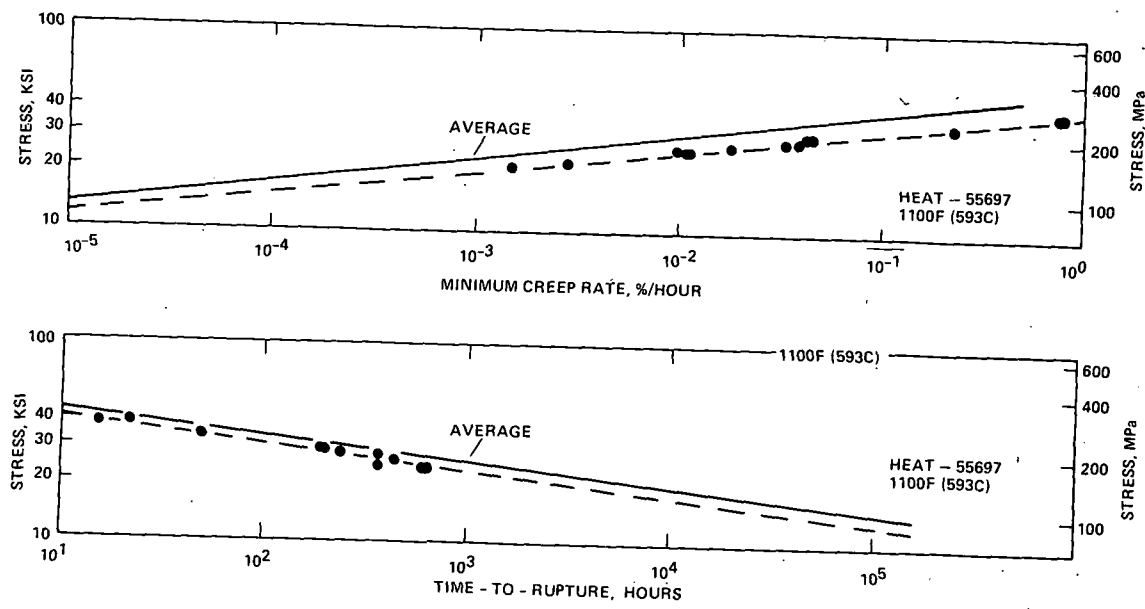


Fig 1

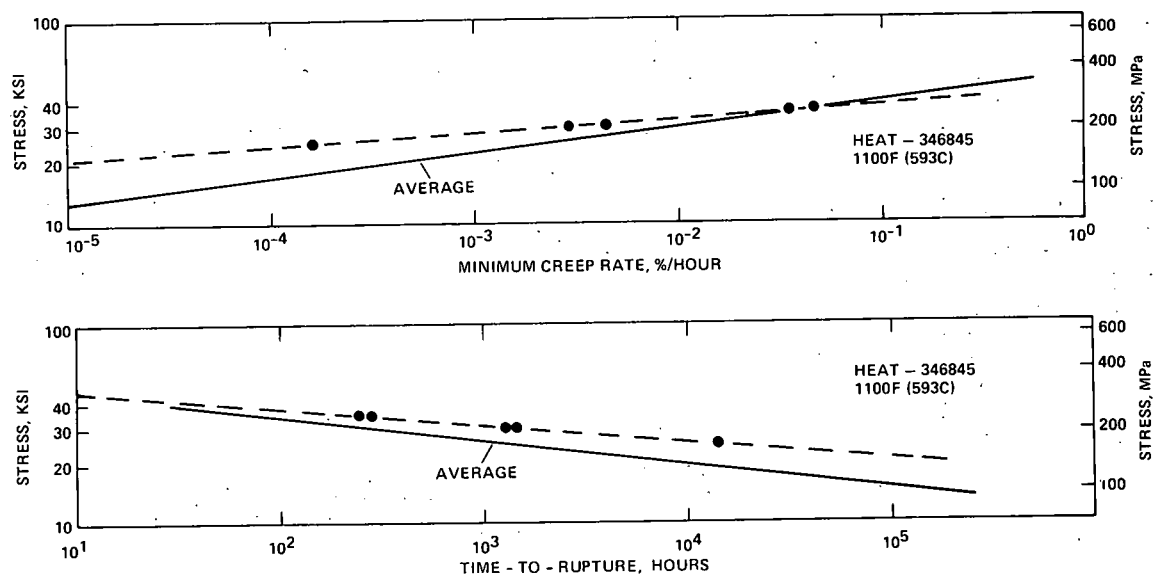


Fig 2

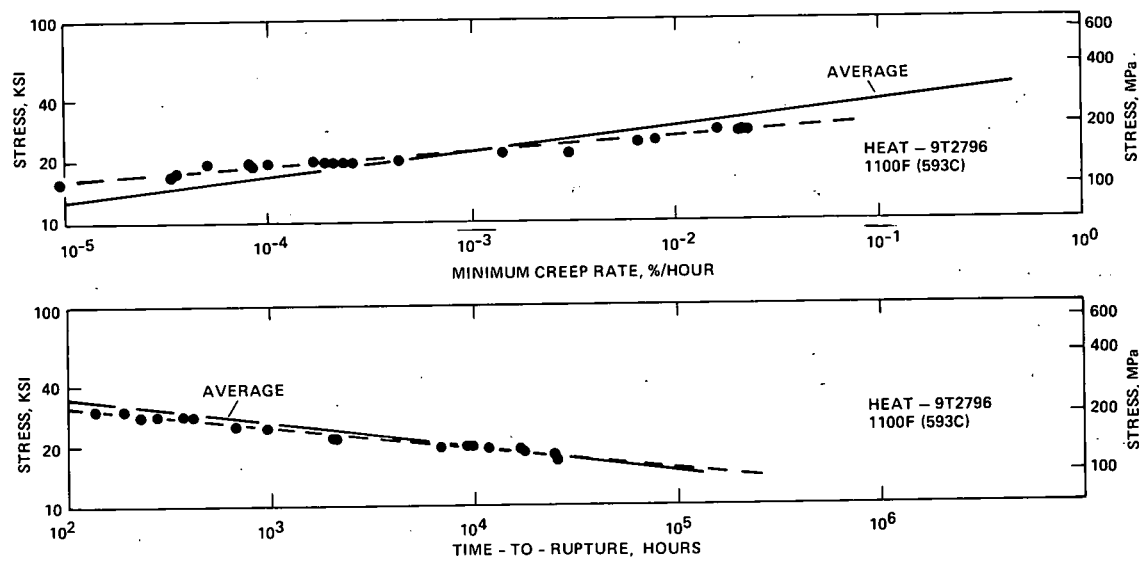


Fig 3

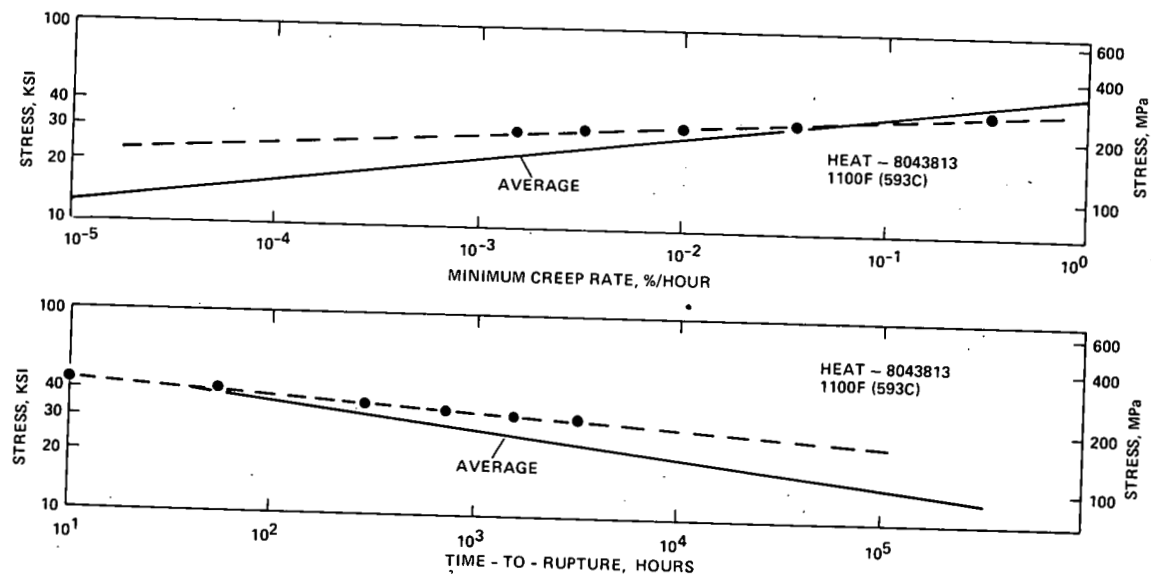


Fig 4

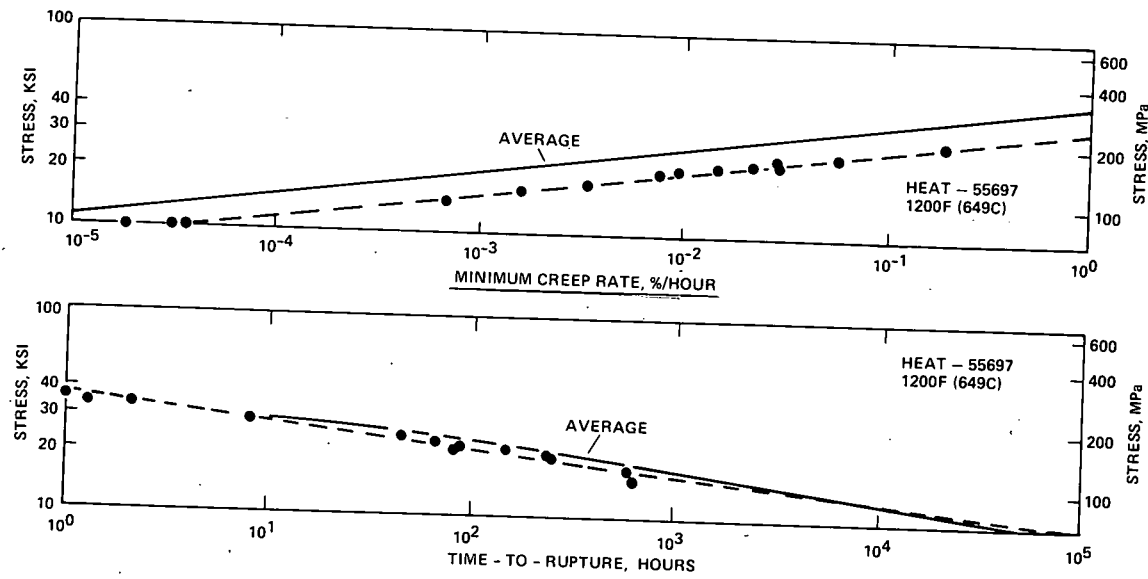


Fig 5

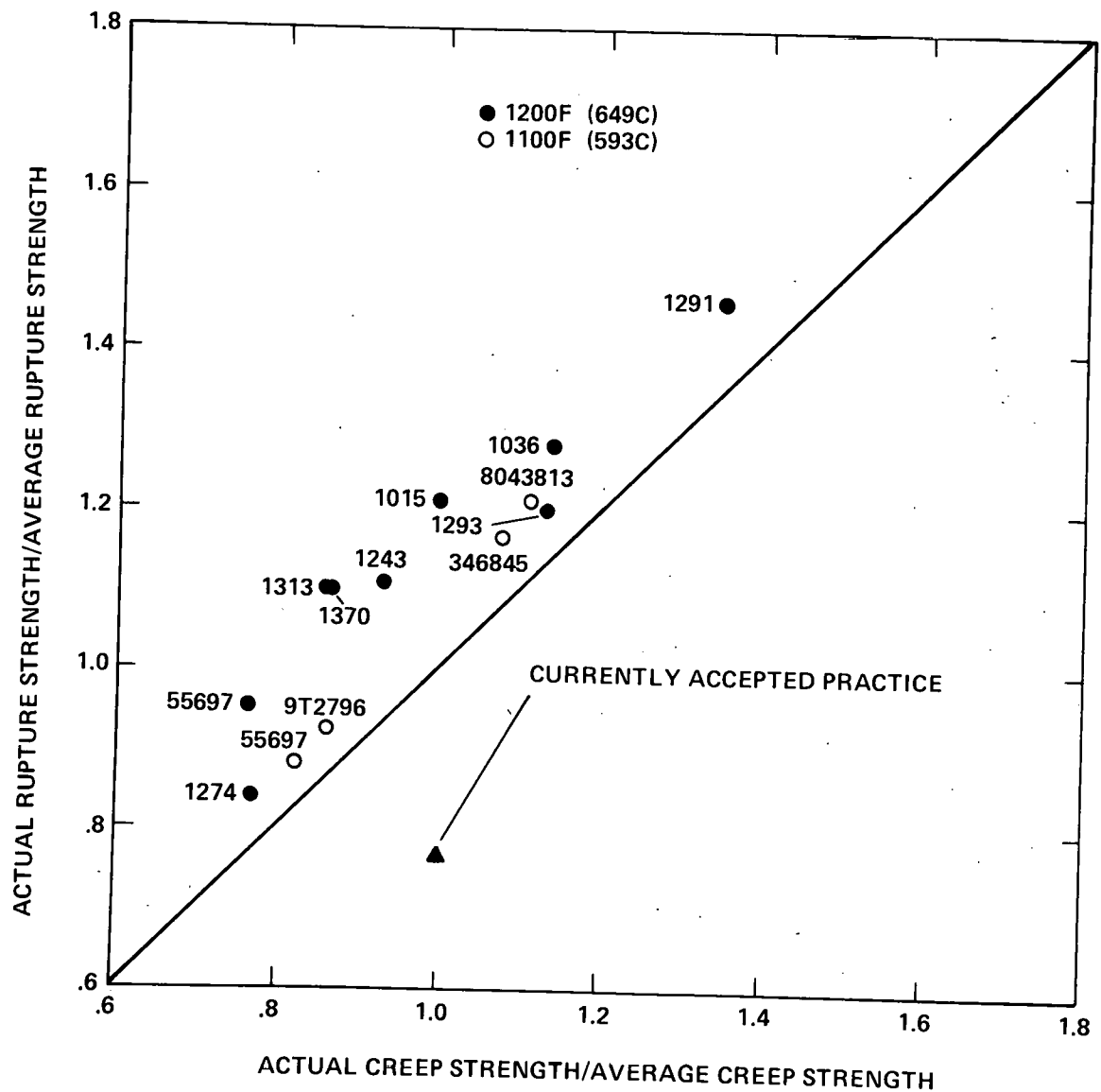


Fig 6

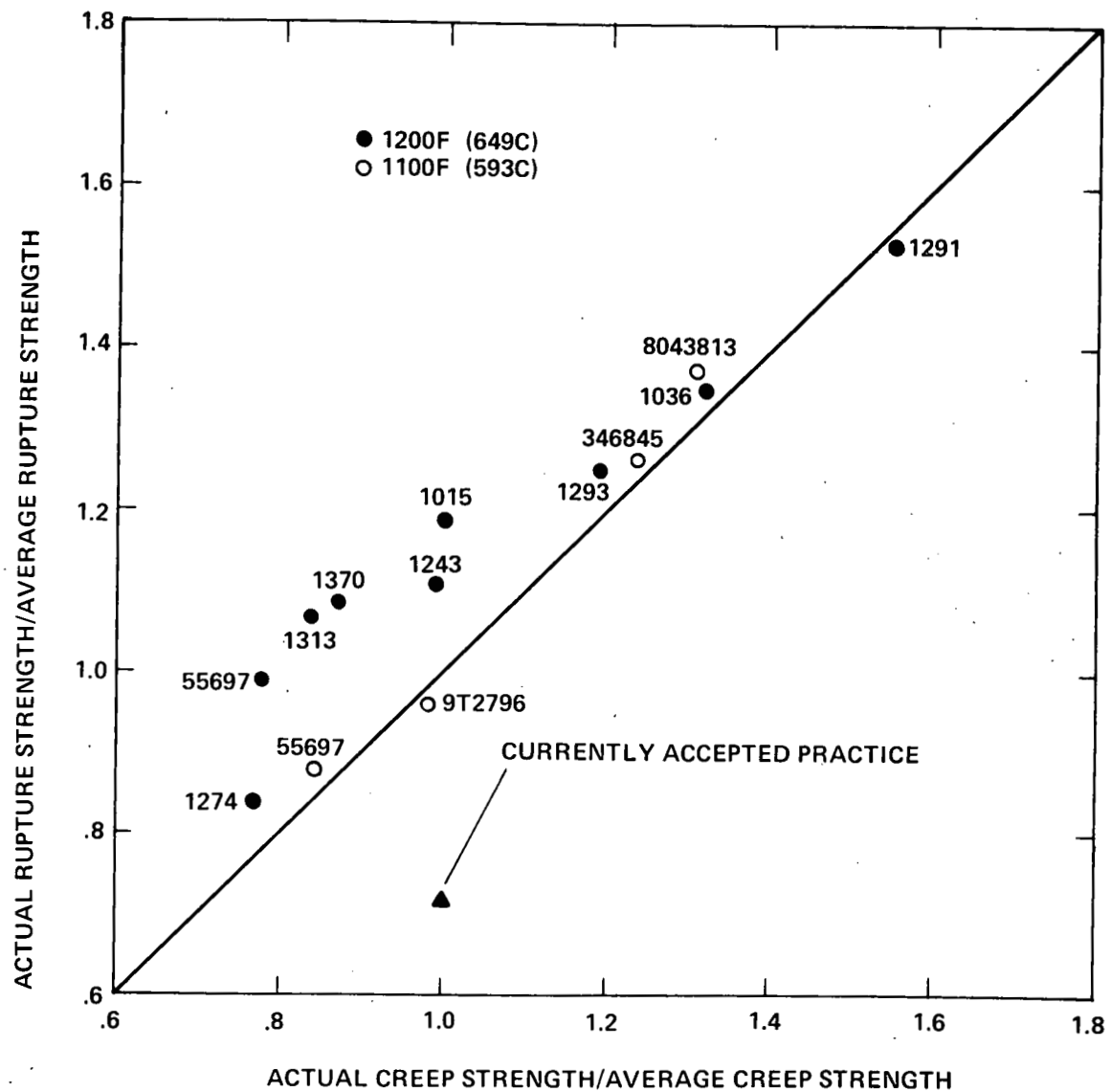


Fig 7

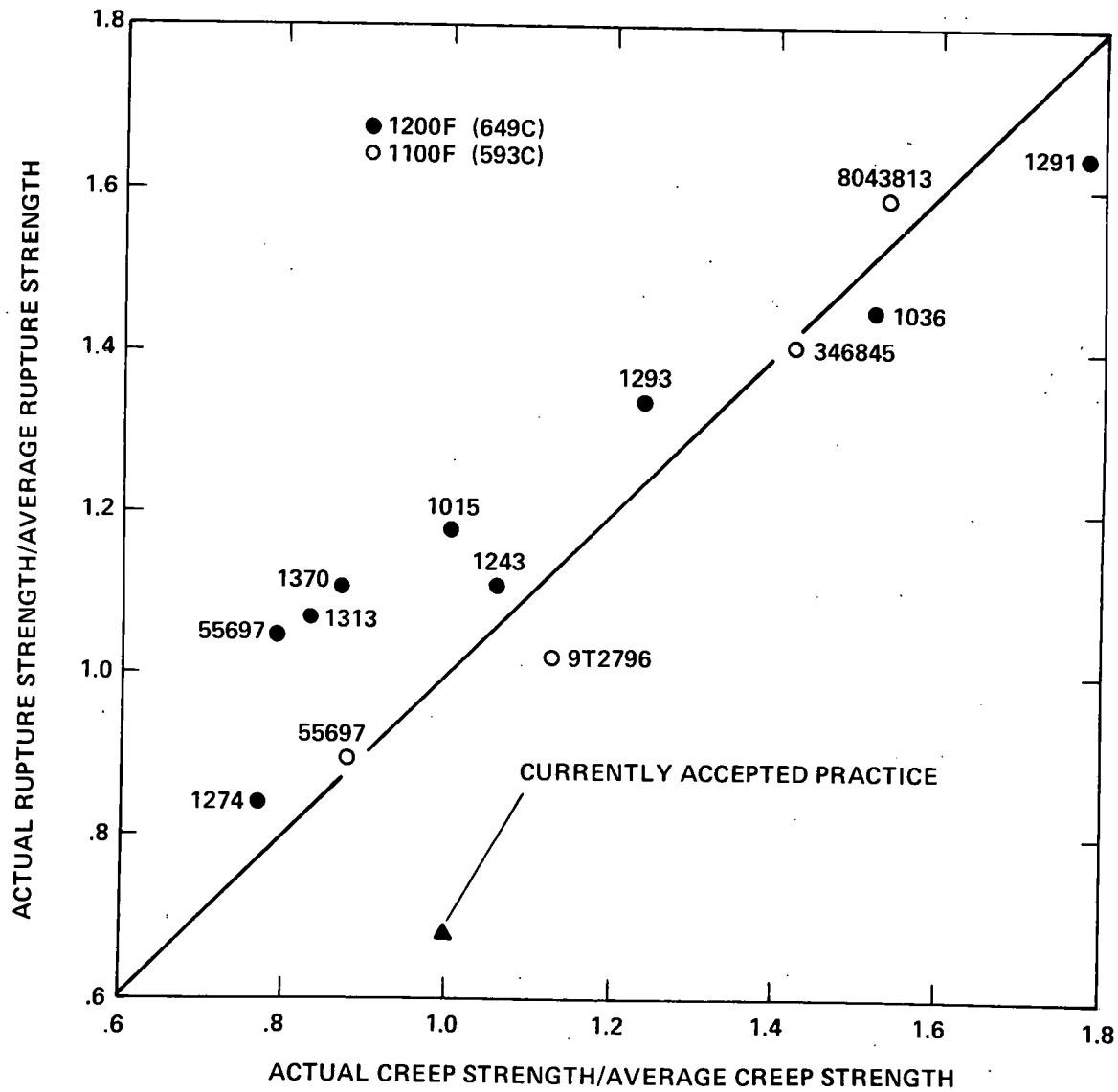


Fig 8

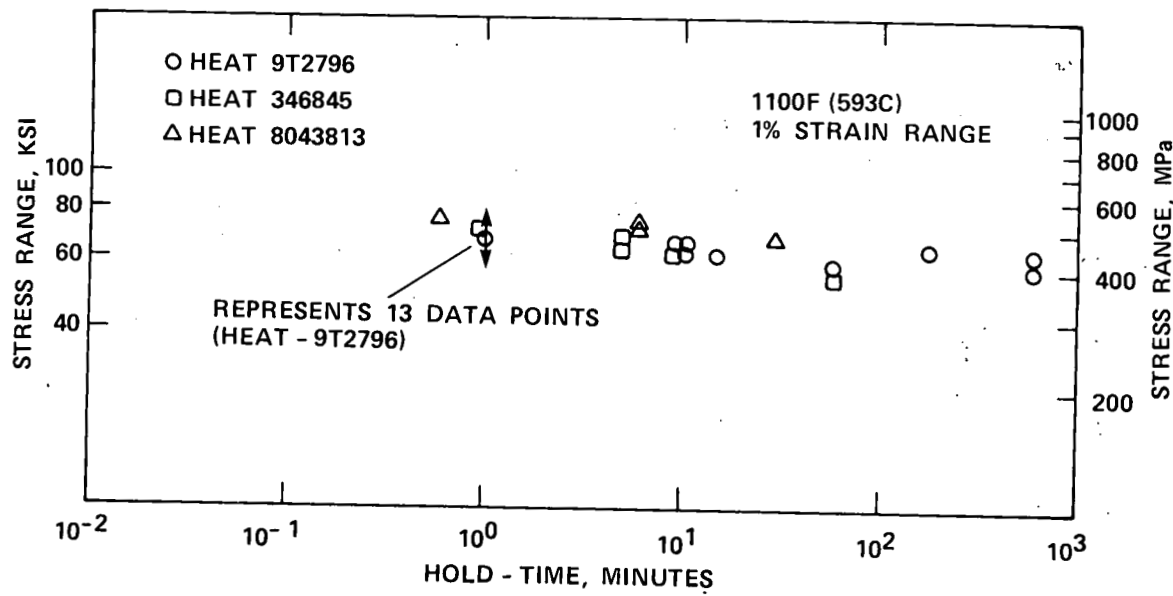


Fig 9

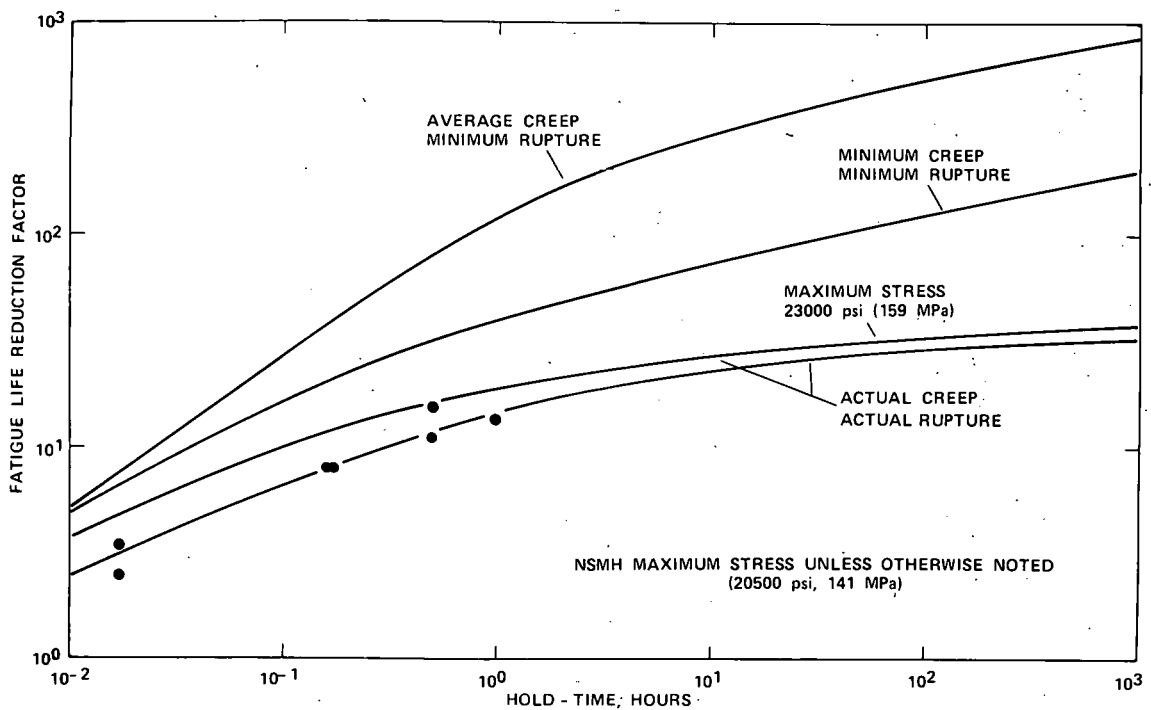


Fig 10

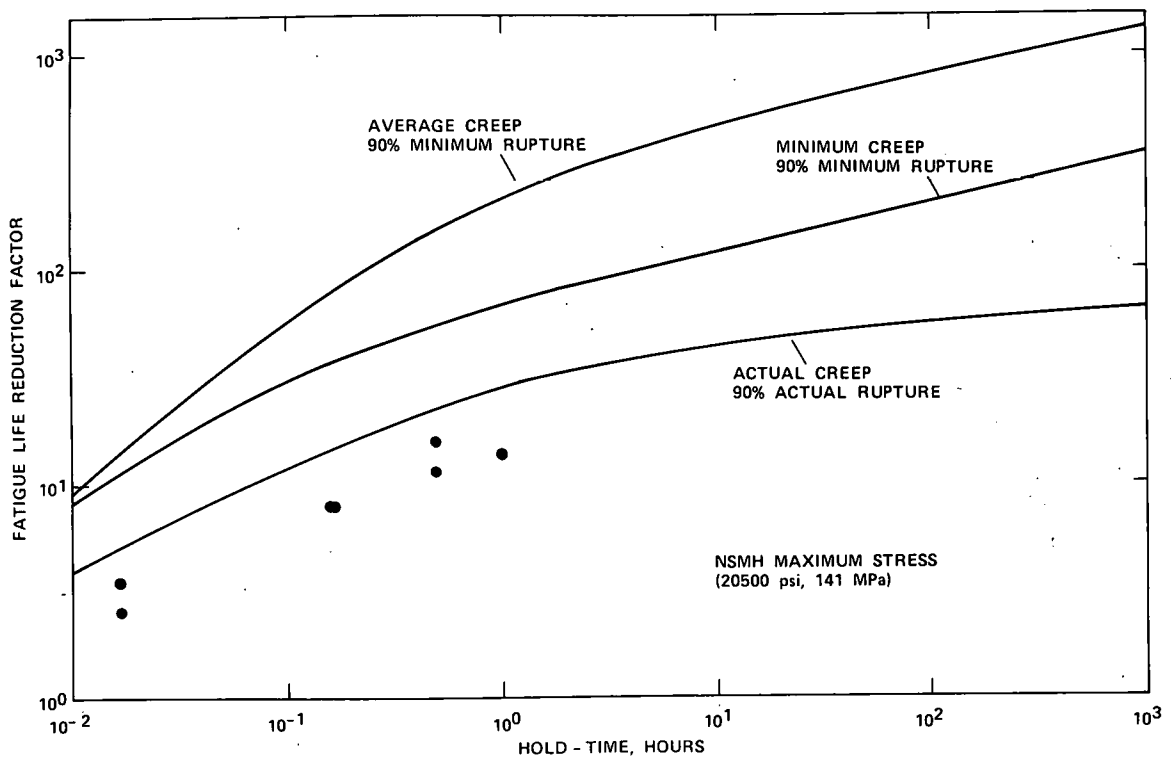


Fig 11

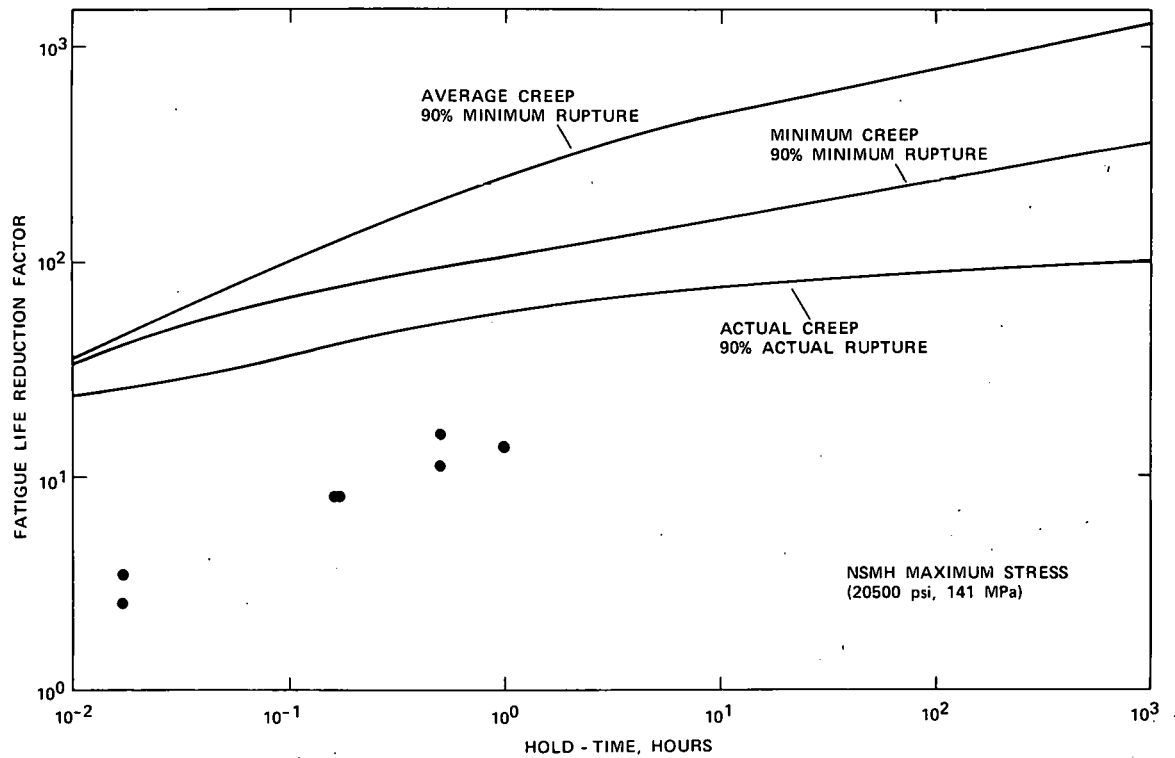


Fig 12

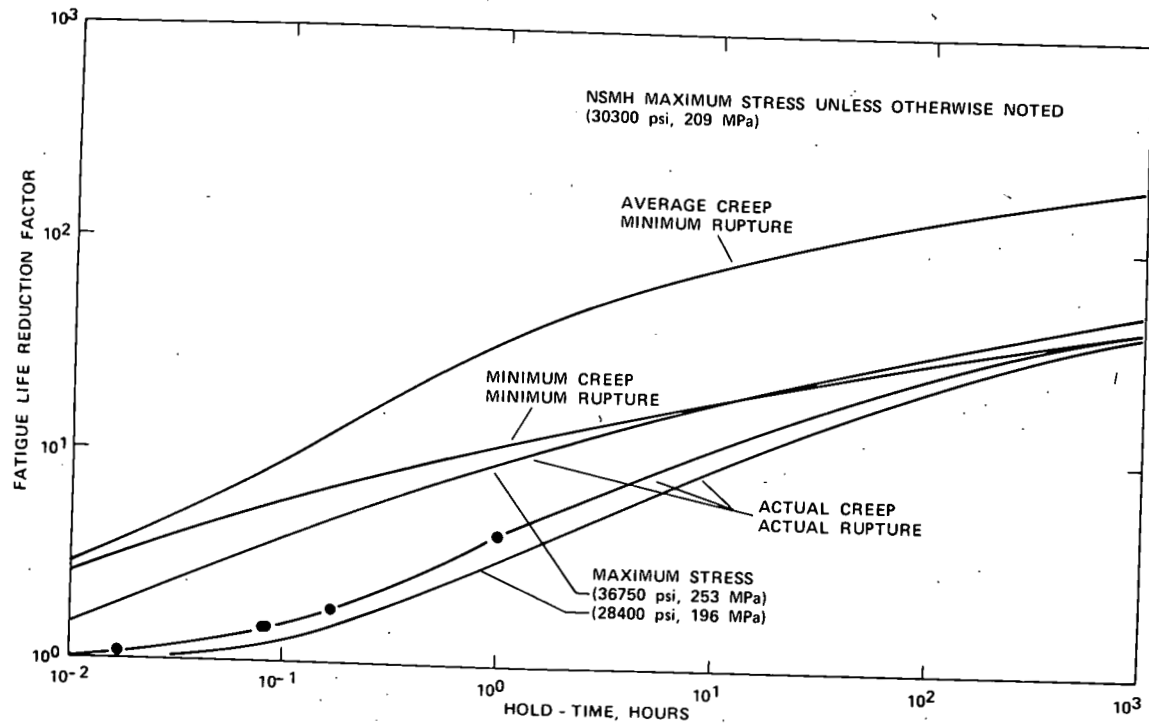
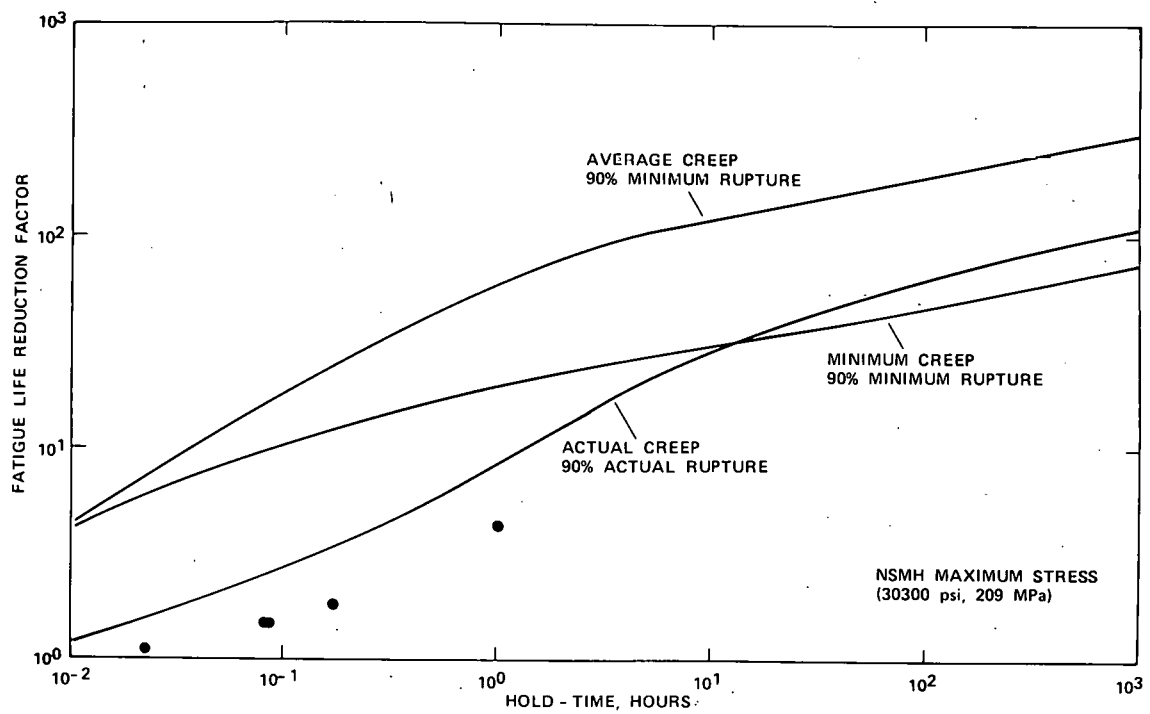
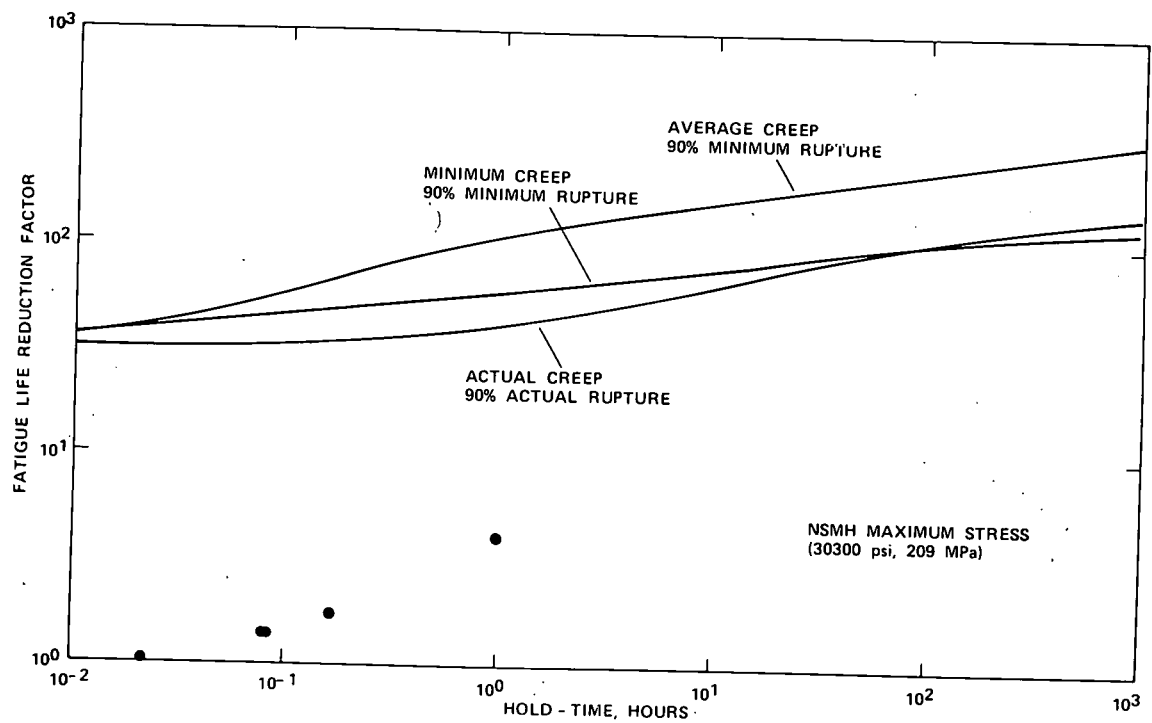


Fig 13



6

15 18



F15 15

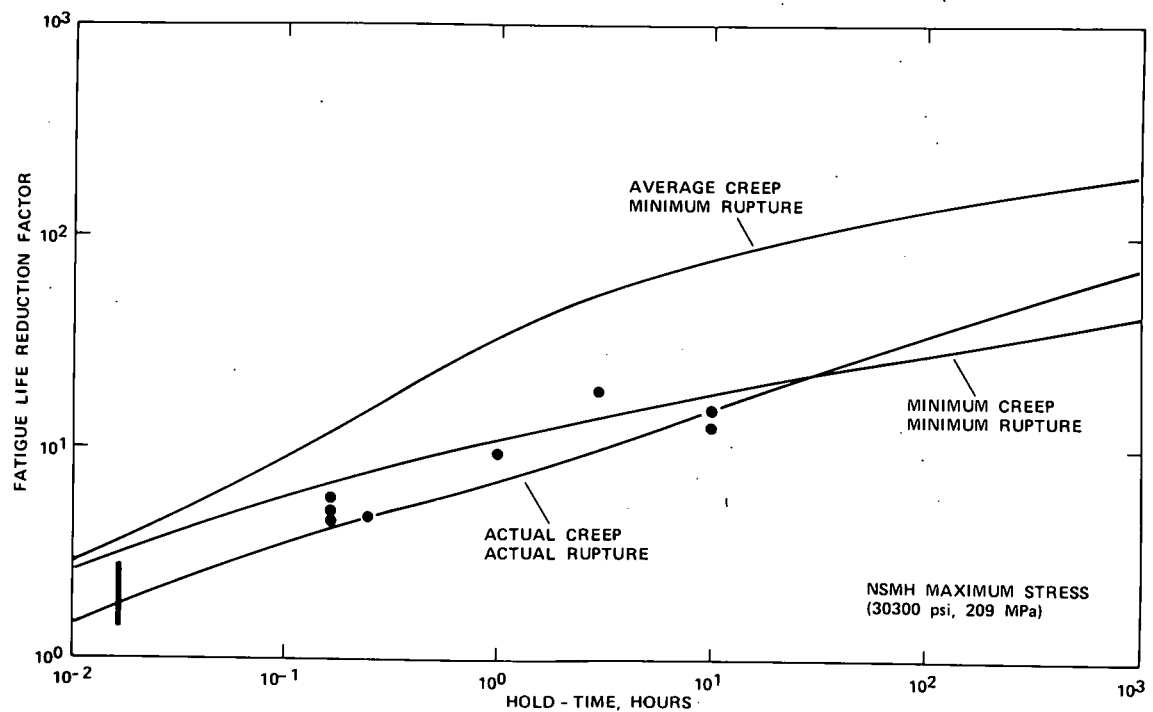


Fig 16

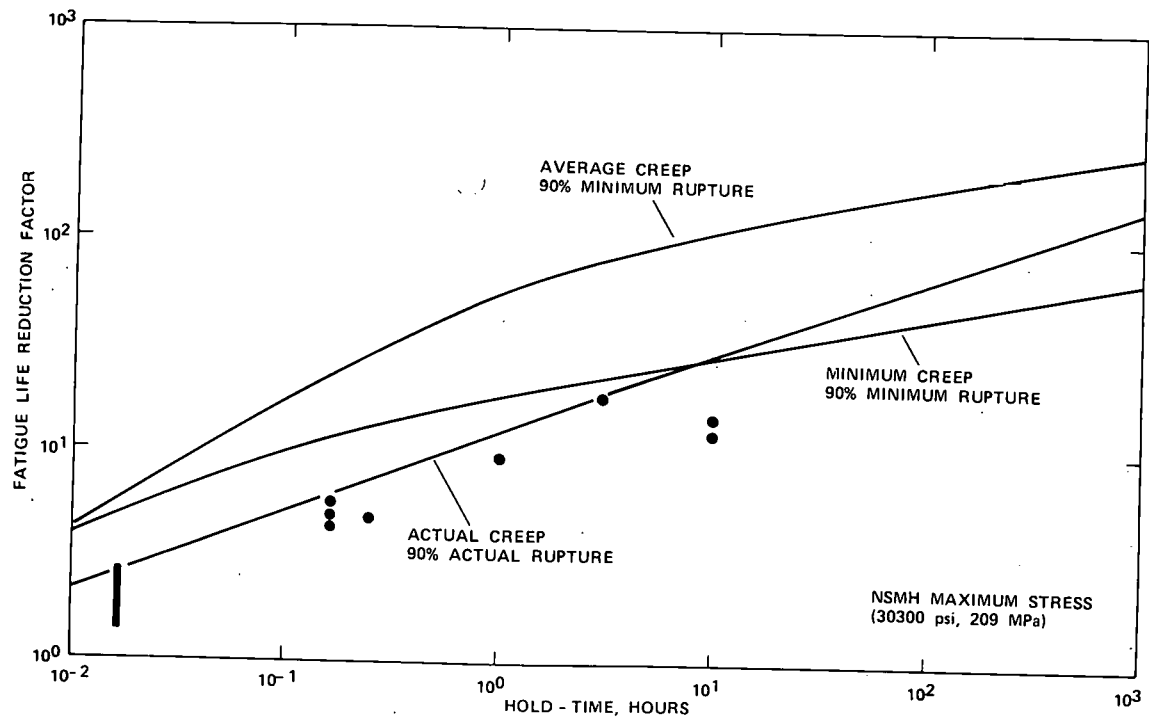
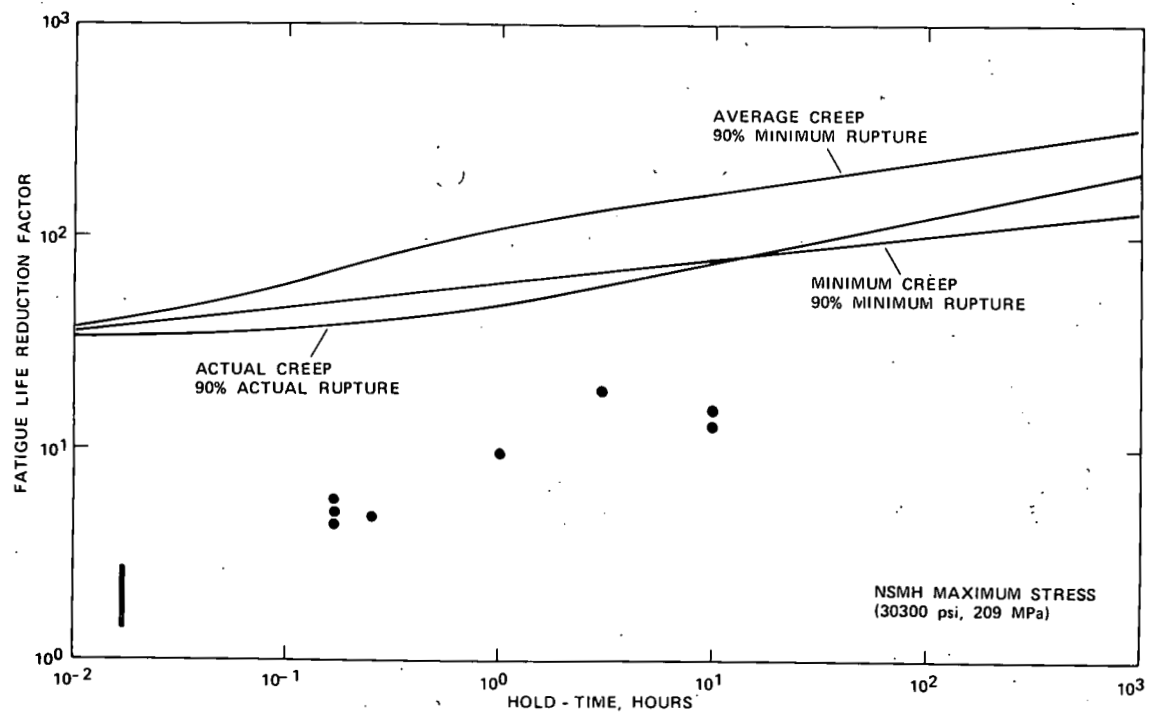


Fig 17



F15 18

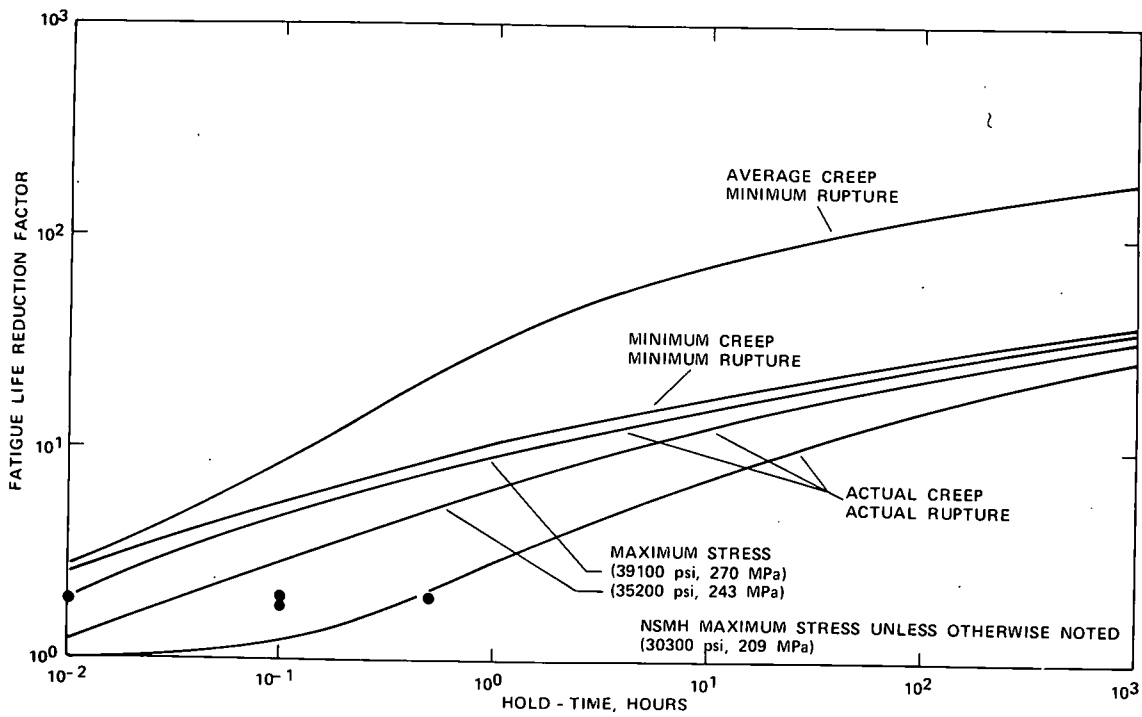
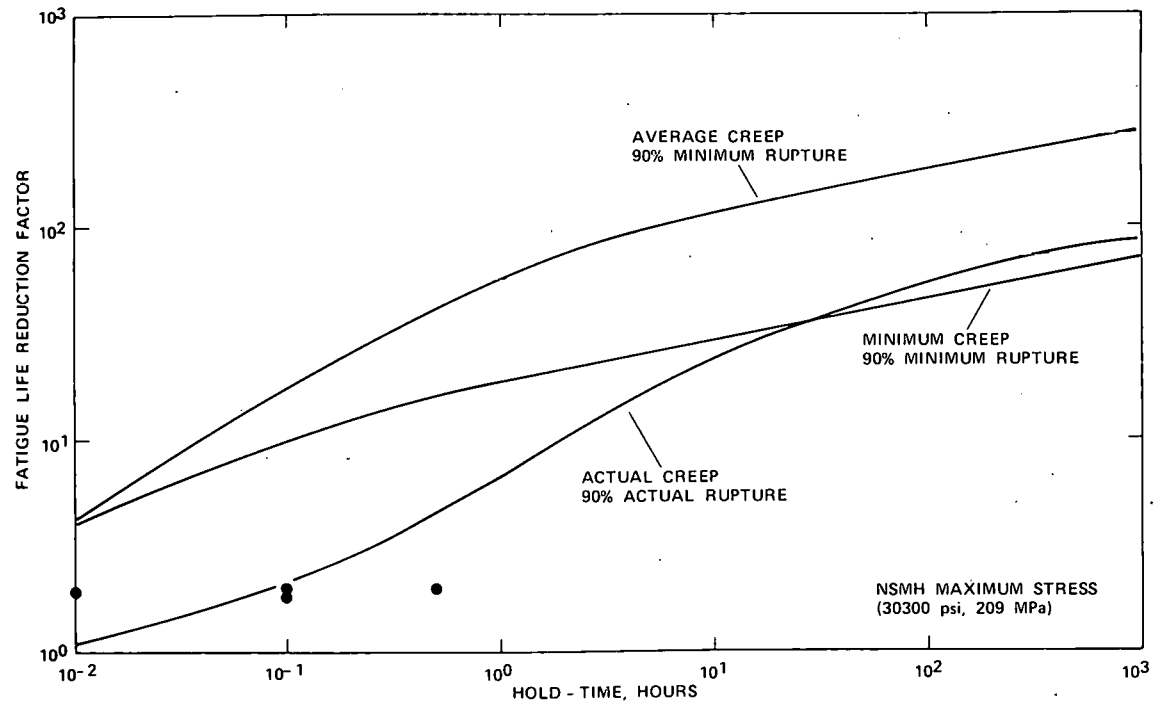
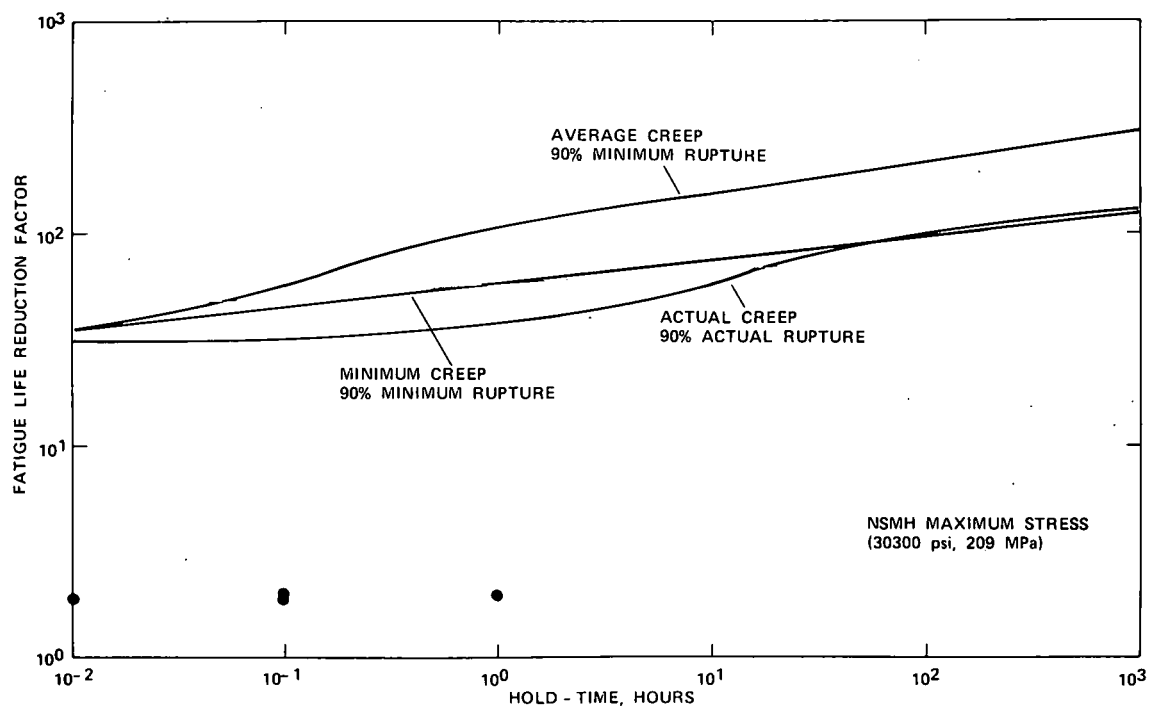


FIG 19

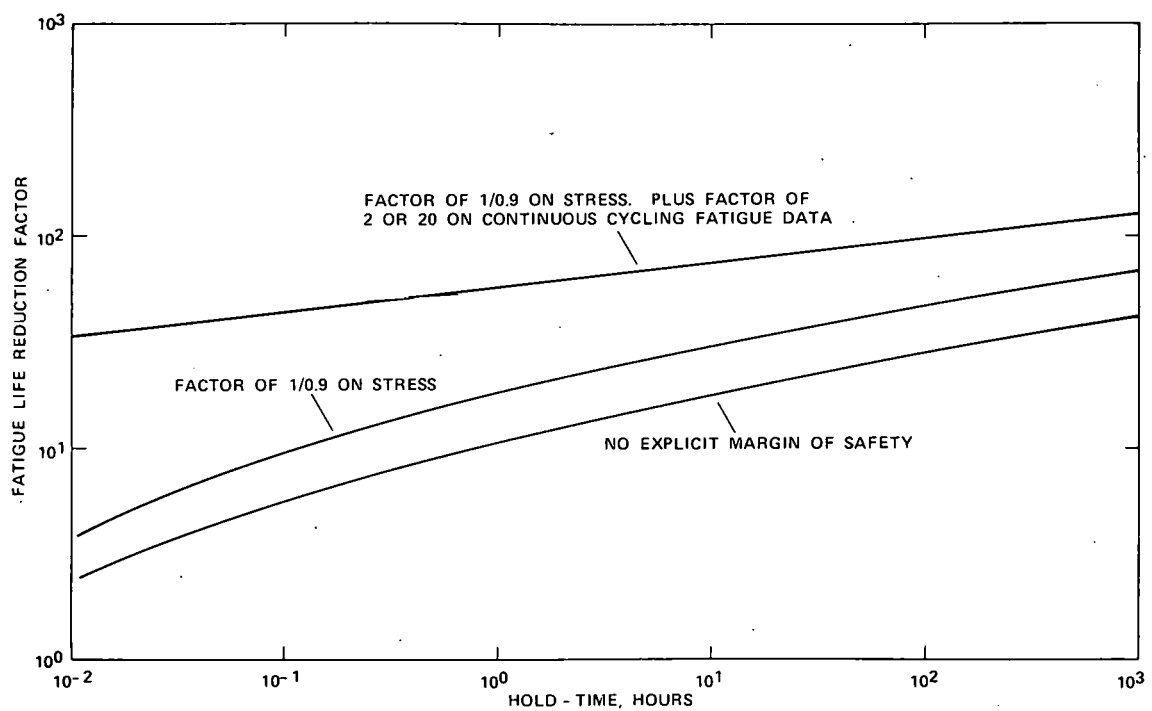


12

Fig 20

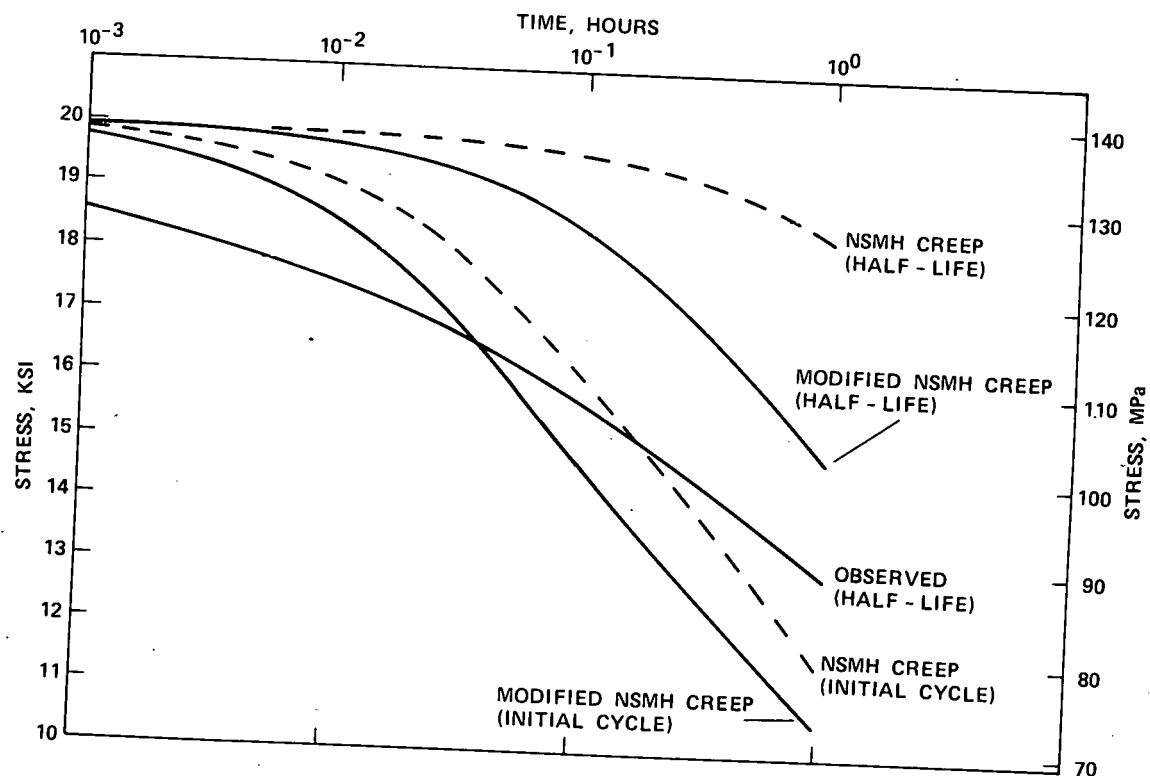


F15 21



12

Fig 22



F15 23

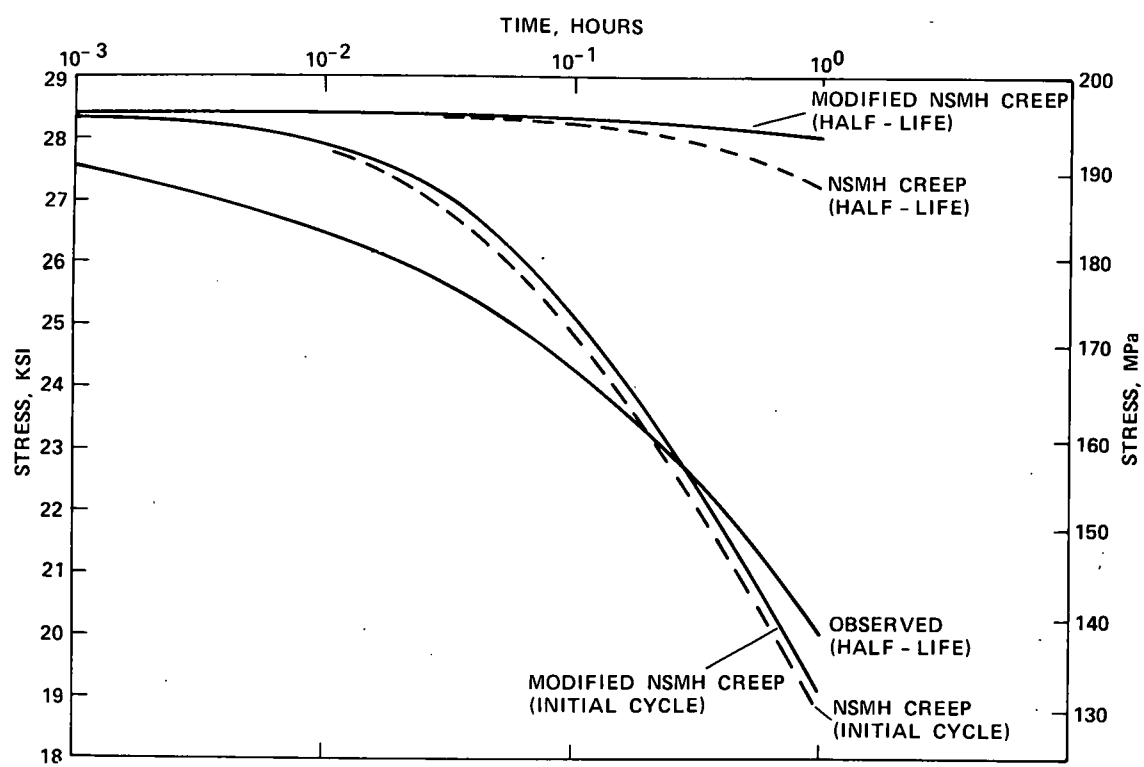
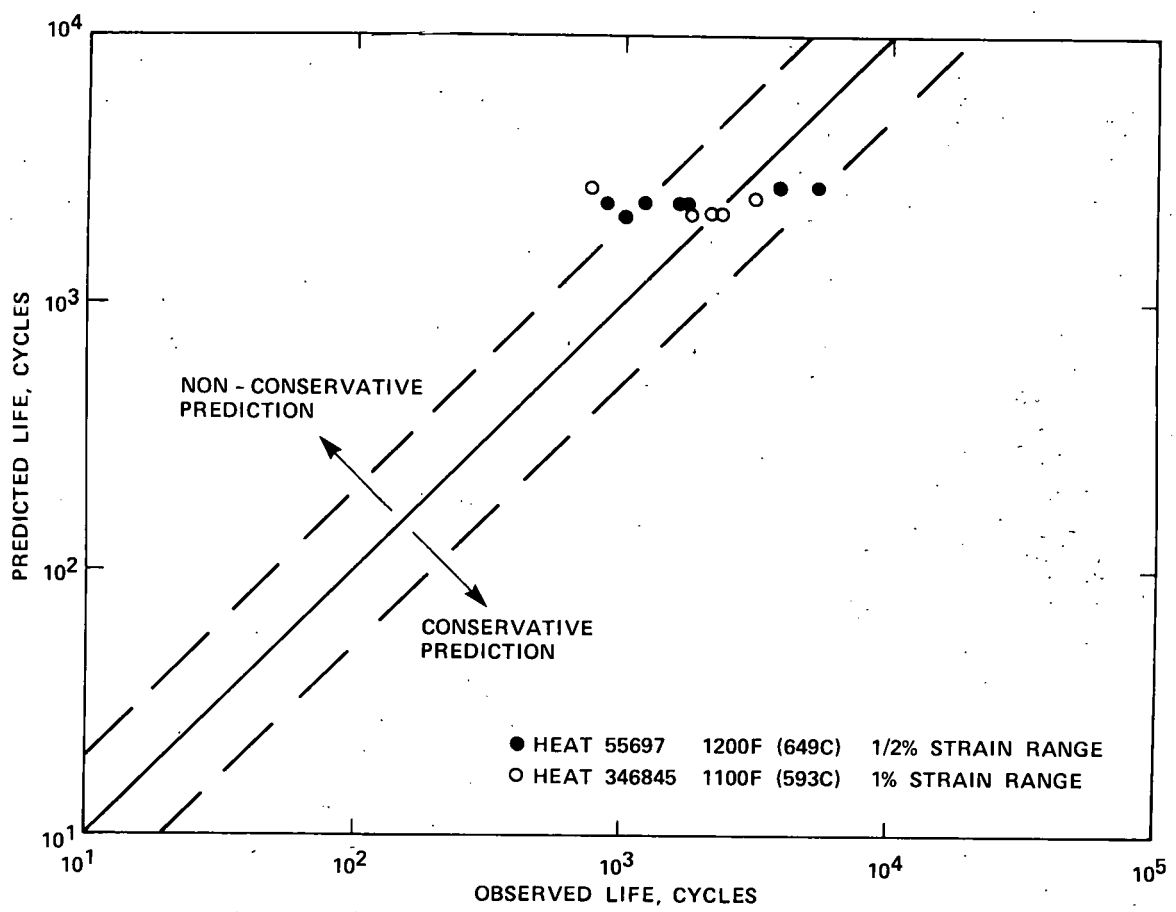
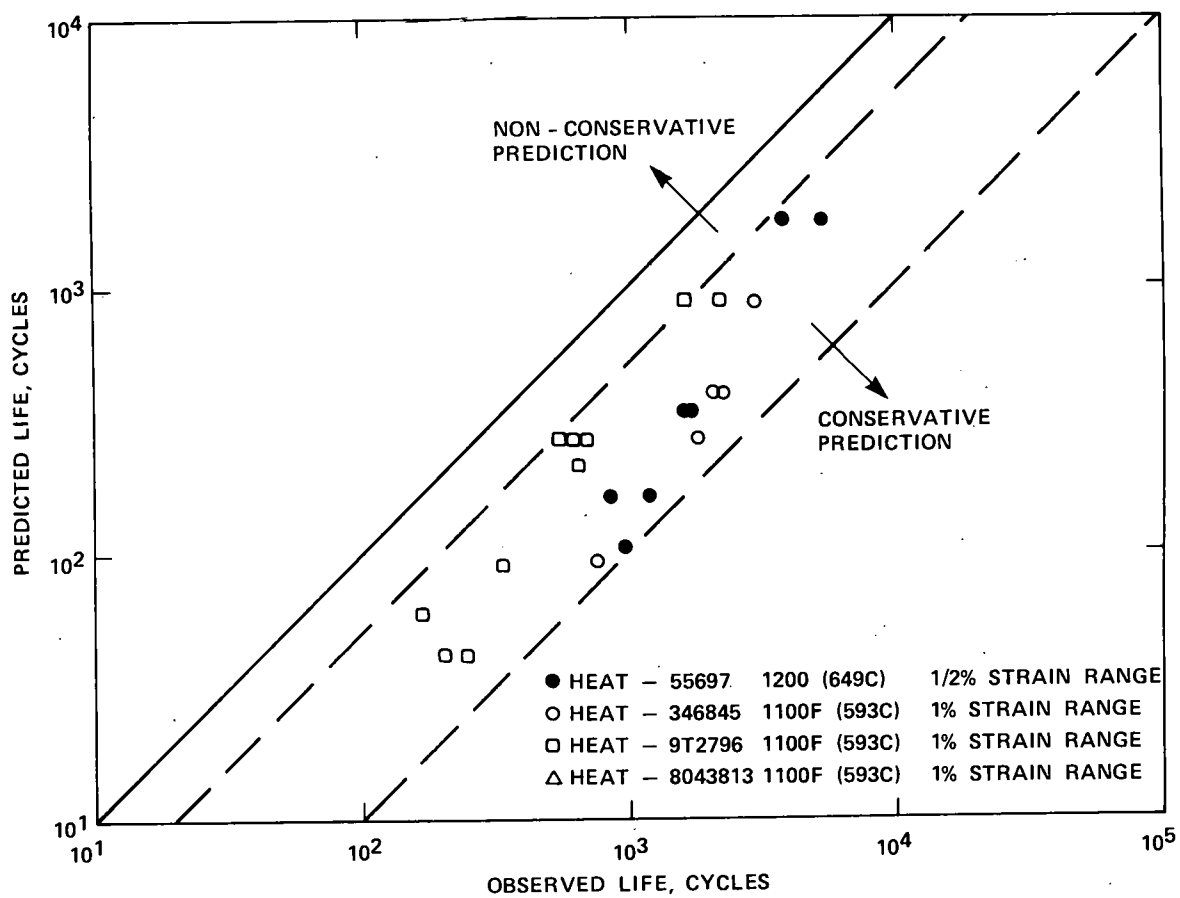


Fig 24



F15 25



F-15 26

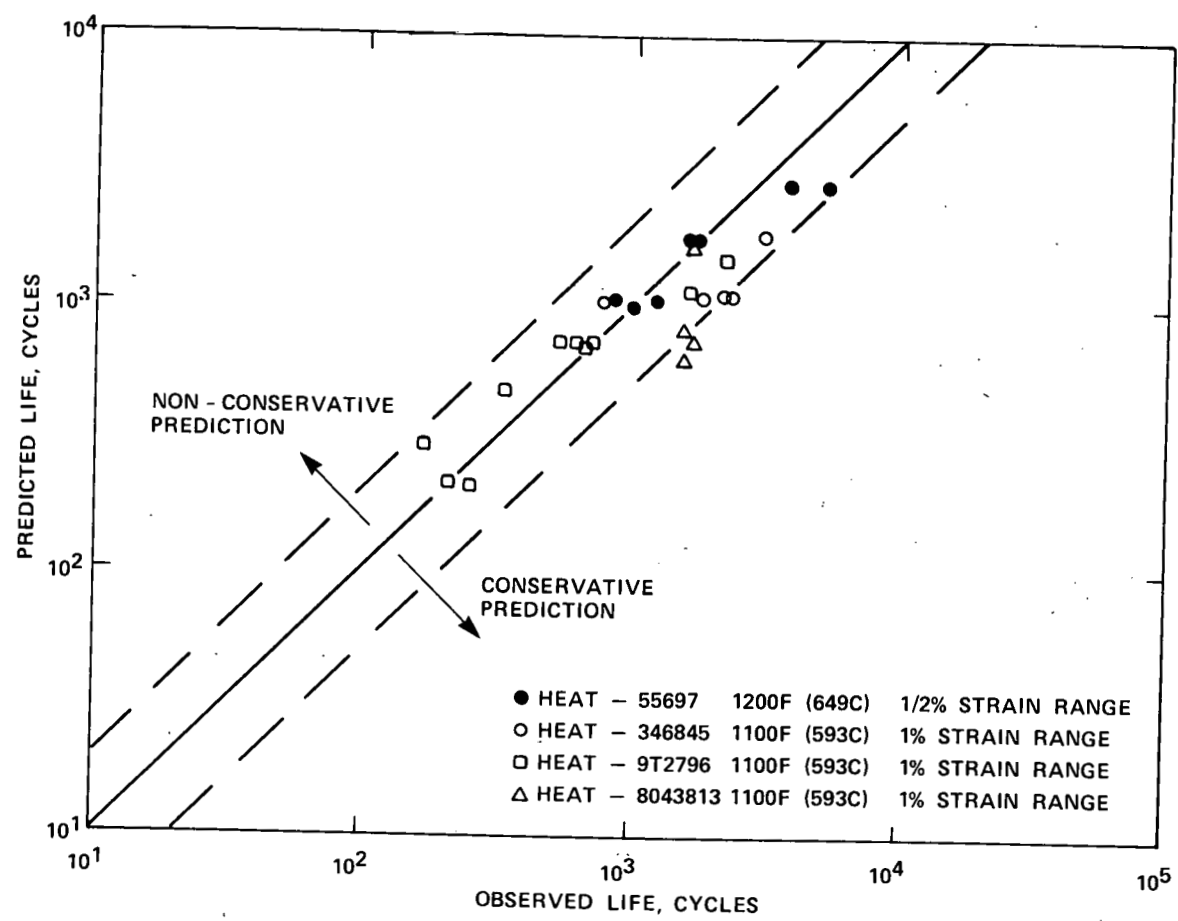
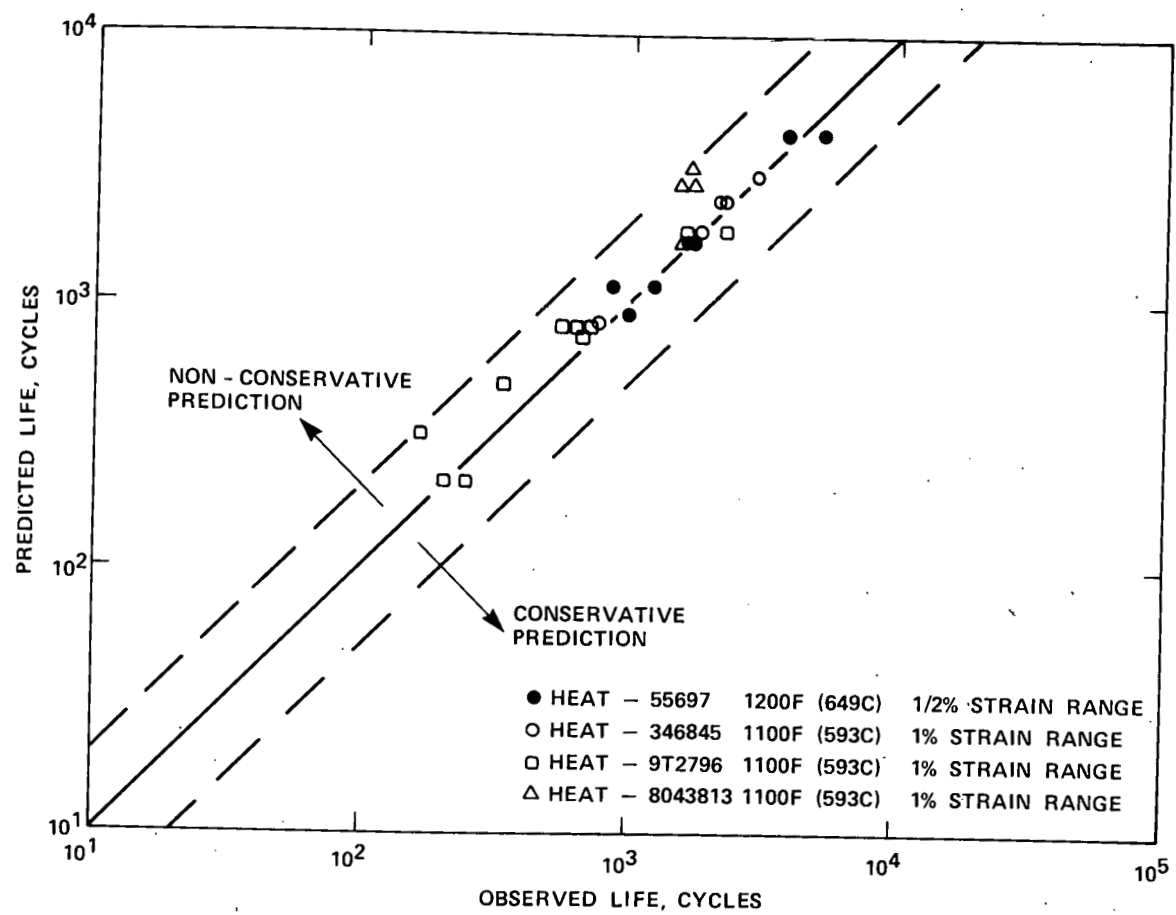


Fig 27



F15 28

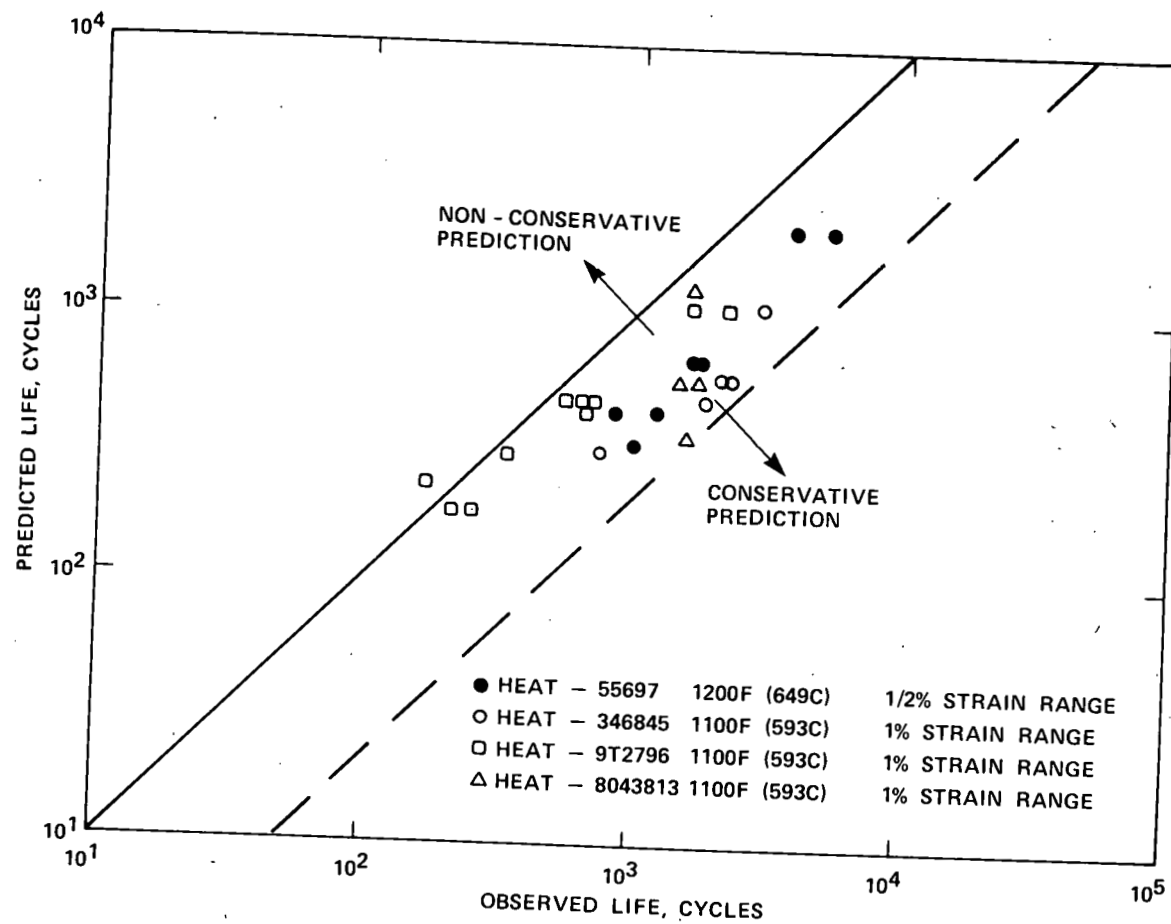


Fig 29